ChemPubSoc Europe

DOI: 10.1002/chem.201504817

CHEMISTRY A European Journal Full Paper

Cyclopropanation Catalyst

Design and Synthesis of Novel Chiral Dirhodium(II) Carboxylate Complexes for Asymmetric Cyclopropanation Reactions**

Frady G. Adly,[b] Michael G. Gardiner,[c] and Ashraf Ghanem*[a]

Abstract: A novel approach to the design of dirhodium(II) tetracarboxylates derived from (*S*)-amino acid ligands is reported. The approach is founded on tailoring the steric influences of the overall catalyst structure by reducing the local symmetry of the ligand's N-heterocyclic tether. The application of the new approach has led to the uncovering of $[Rh_2(S\text{-}^{tert}PTTL)_4]$ as a new member of the dirhodium(II) family with extraordinary selectivity in cyclopropanation reactions. The stereoselectivity of $[Rh_2(S\text{-}^{tert}PTTL)_4]$ was found to be comparable to that of $[Rh_2(S\text{-PTAD})_4]$ (up to >99% *ee*), with the extra benefit of being more synthetically accessible. Correlations based on X-ray structures to justify the observed enantioinduction are also discussed.

Introduction

Dirhodium(II) complexes have been used as effective catalysts for highly stereoselective inter- and intramolecular cyclopropanation reactions.[1] Their superior level of stereoselectivity is such that they can serve as powerful tools for the construction of molecules with complex structures.

Aside from instances in which catalysis optimisation is mapped onto specific structural features of the substrate, development in the field of dirhodium(II) chiral catalysis is related to either electronic or steric modifications within the complex framework.[2] However, researchers in this field rely on exploring and amending the steric profiles and conformations adapted by bridging ligands for the discovery of new catalysts, prediction of transition states, and justification for the observed selectivity.[2] In contrast, the strategy of electronic modification is generally limited to the fine-tuning of the selectivity of a particular catalyst when used in a particular reaction towards the preparation of a particular class of products.[2b]

The most obvious example is Hashimoto and co-workers' phthalimide-based catalytic series. Careful analysis of this series in various reactions reported by Hashimoto and co-workers revealed a trend between the steric bulk at the α position and the enantioselectivity of the catalyst.[3] The enantioselectivity increases with increasing steric bulk and the highest enantioselectivity was observed with $[Rh_2(S\text{-PTTL})_4]$, which carries a *tert*-butyl group (Figure 1).

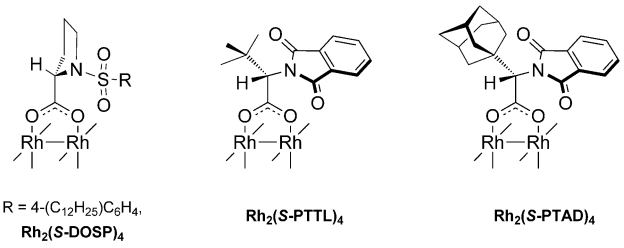

Figure 1. Available highly stereoselective dirhodium(II) carboxylates.

Later, Davies and co-workers extended the idea and assumed that a catalyst carrying the more bulky adamantyl moiety at the α-carbon atom would surpass those carrying the standard PTTL ligands (Figure 1).[4] $[Rh_2(S\text{-PTAD})_4]$ demonstrated enhanced levels of enantioselectivity and acted as a complementary catalyst when $[Rh_2(S\text{-DOSP})_4]$ failed to give high asymmetric induction with some of donor–acceptor systems.[5] In addition, $[Rh_2(S\text{-PTAD})_4]$ was reported to be the optimal chiral catalyst when the acceptor group in the donor–acceptor substrates is a phosphonate ester,[4] nitrile,[6] trifluoromethyl[7] or keto[8] group, giving better enantioselectivities than $[Rh_2(S\text{-PTTL})_4]$. In fact, the emergence of $[Rh_2(S\text{-PTAD})_4]$ circumvented to a great extent the limitations of selectivity associated with $[Rh_2(S\text{-DOSP})_4]$. However, the synthesis of the (*S*)-PTAD ligand is based on (*S*)-α-adamantylglycine, which is not commercially available and its asymmetric synthesis is very tedious and tiresome.[4] These problems associated with ligand preparation have blemished the overall interest in this catalyst.[9]

[a] *Dr. A. Ghanem*
Biomedical science department
University of Canberra
ACT, 2601 (Australia)
E-mail: ashraf.ghanem@canberra.edu.au

[b] *Dr. F. G. Adly*
University of Canberra
ACT, 2601 (Australia)

[c] *Dr. M. G. Gardiner*
School of Physical Sciences, ChemistryUniversity of Tasmania
Hobart, TAS, 7001 (Australia)

[**] *The catalyst ($[Rh_2(S\text{-}^{tert}PTTL)_4]$; patent PCT/AU2015/000557) is now available at STREM Chemicals.*

Supporting information and ORCID(s) from the author(s) for this article are available on the WWW under http://dx.doi.org/10.1002/chem.201504817.

In the same context, symmetry is believed to be an important concept that plays an extensive role in chiral catalysis. The use of high-symmetry catalysts is assumed to minimise the number of possible substrate trajectories in the catalytic steps of the reaction in question. This, in turn, can afford a predictable, more precise, 3D transition-state structure. So, generally, in the field of chiral catalyst design, the use of ligands with the highest possible symmetry is usually preferred to generate high-symmetry catalysts. The use of such ligands can significantly simplify the prediction of stereoinduction mechanisms. Moreover, the synthesis of such ligands, in most cases, is much simpler.[10]

For dirhodium(II) carboxylate complexes, the paddlewheel framework provides a distinguishable scaffolding for achieving higher-symmetry chiral complexes through what is called a "modular approach".[2a] In this approach, several identical C_1-symmetric ligands surround the inherently high-symmetry core to afford a far superior symmetrical homochiral molecule compared with the individual ligand itself. It was believed that chiral dirhodium(II) complexes exhibit exceptionally high stereoselectivities because of this interesting attribute.[2a] However, Fox[11] and Charette[12] and their co-workers independently explored the interruption of this high-symmetry framework. They replaced one of the ligands with an achiral ligand, which led to the generation of lower-symmetry heteroleptic complexes. The results of screening tests revealed that lowering the global symmetry of the catalysts had a beneficial impact on their asymmetric induction.

For dirhodium(II) catalysts derived from N-protected amino acid ligands, it has long been held (based on the enantioselectivities achieved with these systems) that N-aryl tethers can act as steric blockers. The role of these tethers is considered pivotal in controlling the trajectory of the incoming substrates during catalysis. Following the classical catalyst design described above, all the reported dirhodium(II) complexes belonging to this family have a C_{2v}-symmetric N-heterocyclic tether for the construction of the chiral ligands.

In 2004, Müller and Ghanem[13] reported several [Rh_2(*S*-NTTL)$_4$] analogues in which only one hydrogen in the heterocyclic tether is substituted, generating ligands carrying C_s-symmetric N-protecting groups (Figure 2). Their results revealed that the [Rh_2(*S*-4-Br-NTTL)$_4$]-catalysed cyclopropanation of styrene with dimethyl malonate proceeded with far improved levels of enantioselectivity (82% *ee*) compared with its parent complex [Rh_2(*S*-NTTL)$_4$] (37% *ee*).[13a,14] The same catalyst was also effective in olefin cyclopropanation with Meldrum's acid giving 92% *ee* with styrene and 87% *ee* with pent-1-ene.

Very recently, our group explored this further and reported [Rh_2(*S*-1,2-NTTL)$_4$] as a new member of the chiral dirhodium(II) family derived from C_s-symmetric N-protected *tert*-leucine (Figure 2). The idea was to reduce the local symmetry of the ligand's heterocyclic tether in [Rh_2(*S*-1,2-NTTL)$_4$] by fusing a ring at one side of the N-heterocyclic tether. The results demonstrated that [Rh_2(*S*-1,2-NTTL)$_4$] is a promising catalyst for the cyclopropanation reactions involving donor–acceptor phosphonate carbenoids, however, the results did not show a clear advantage of the "lower-symmetry" approach.[15] As a consequence, two more approaches were investigated as improved methods for reducing the local symmetry of the ligand's heterocyclic tether.

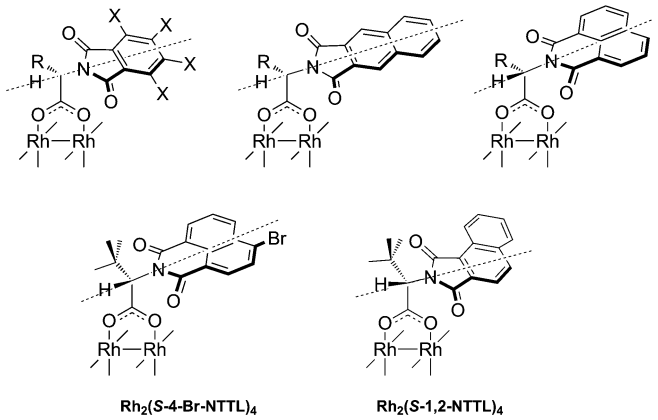

Figure 2. Comparison of the backbone structure of the ligands in dirhodium(II) complexes.

Guided by previous findings relating to the nature of the chiral crown cavity in dirhodium(II) complexes,[13b,16] we have continued to modify the N-heterocyclic tether of ligands derived from L-*tert*-leucine as a pivotal part of this type of ligands. The aim of the study reported herein was to explore in depth the effect of reducing the local symmetry of the N-heterocyclic tether and to trace its effect on the mechanism of stereoselection in asymmetric cyclopropanation reactions.

Results and Discussion

New ligands **1**–**4** carrying N-protecting groups of reduced C_s symmetry were prepared as illustrated in Scheme 1. Standard ligand-exchange conditions between the prepared ligands and [Rh_2(OAc)$_4$] generated [Rh_2(*S*-1-Ph-BPTTL)$_4$] (**5**), [Rh_2(*S*-^{tert}PTTL)$_4$] (**6**), [Rh_2(*S*-BOTL)$_4$] (**7**) and [Rh_2(*S*-BHTL)$_4$] (**8**) as green solids in yields of 67, 71, 92 and 83%, respectively (Scheme 2). These four catalysts emerged as a result of applying alternative strategies for lowering the symmetry of the N-heterocyclic tether.

Similar to the case of the *N*-1,2-NTTL ligand reported earlier,[15] partial substitution of the ring can reduce the symmetry of the N-protecting group, as in the case of [Rh_2(*S*-1-Ph-BPTTL)$_4$] (**5**) and [Rh_2(*S*-^{tert}PTTL)$_4$] (**6**). This is due to the removal of the mirror planes lying both in the heterocyclic plane and perpendicular to this plane. The planarity of the heterocyclic section is maintained in these two complexes, but the local symmetry of the N-protecting group is reduced from C_{2v} to C_s by virtue of the substituents; *tert*-butyl and phenyl substituents were chosen for their bulk.[17]

As illustrated in Figure 3a, introducing a substituent at either position 3 (3′) or 4 (4′) in the PTTL-derived catalyst **6** will reduce the symmetry of the phthalimide protecting group. But to gain the advantage of the "cavity rim steric impedance effect",[13b] introduction of the substituent at position 4 (4′) was favoured over position 3 (3′). For the BPTTL-derived catalyst **5** (Figure 3b), positions 4 (4′) and 5 (5′) are far away from the

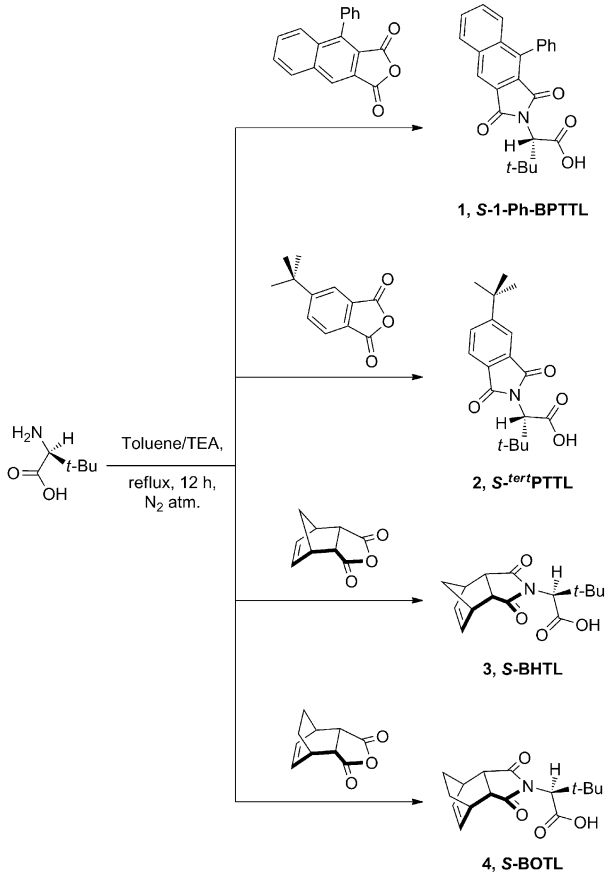

Scheme 1. Preparation of chiral ligands **1**–**4**.

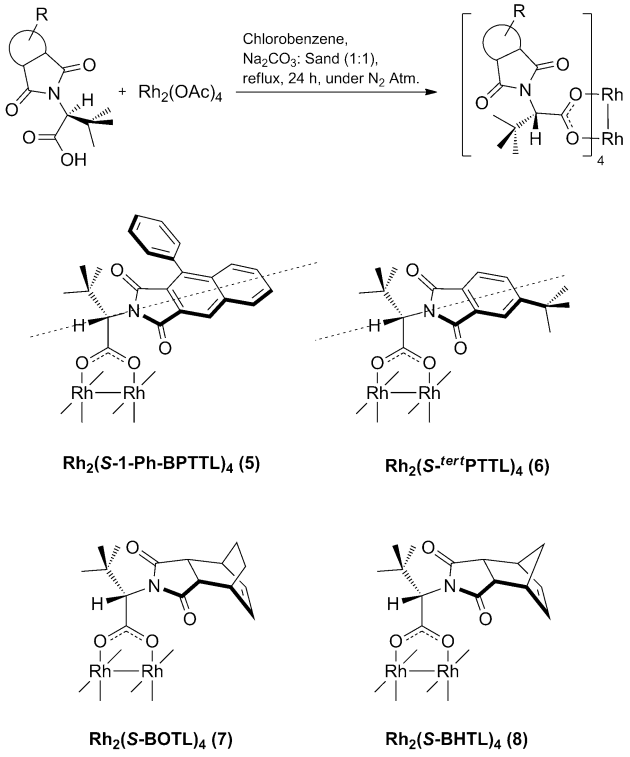

Scheme 2. Synthesis and structures of the complexes **5**–**8**.

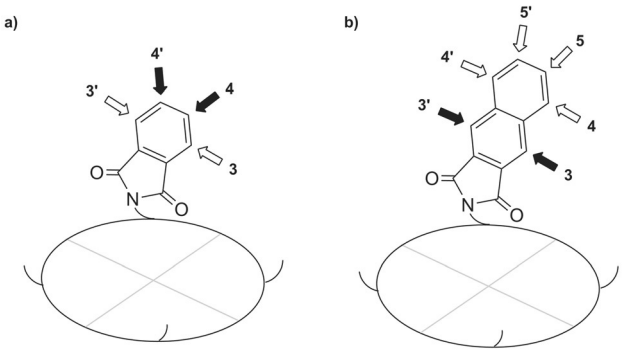

Figure 3. Suitable positions for the introduction of substituents into complexes a) **6** and b) **5**. The favoured positions of substitution are represented by black arrows.

rhodium reactive centre and the introduction of the substituent at any of these two spots is expected to exert minimal influence on the stereoselectivity of the catalyst. As a consequence, introduction of the substituent at position 3 (3′) was favoured. However, the expected "lean" of the nitrogen tether by its clockwise twist will render inequivalent positions 4 and 4′ in **6** (Figure 3a) and positions 3 and 3′ in **5** (Figure 3b). Thus, the anticipated "best" orientation of the substituent was difficult to predict at this stage.

We were very fortunate to find 4-*tert*-butylphthalic anhydride and 1-phenylnaphthalene-2,3-dicarboxylic anhydride to be commercially available, and these were chosen for protection of the *tert*-leucine amino group. Using a commercially available anhydride definitely simplifies the preparation process and makes the final catalyst more synthetically accessible.

In contrast, the reduction of symmetry achieved in [Rh_2(*S*-BOTL)$_4$] (**7**) and [Rh_2(*S*-BHTL)$_4$] (**8**) complexes was quite interesting. The N-protecting group again has C_s symmetry, which means that all four N-protecting groups could be equivalently positioned around the extremity of the chiral crown cavity and not reduce the C_4 symmetry of the final complex. To the best of our knowledge, no catalyst structure has been reported in which the rotation of ligand rings results in a different size chiral cavity (Figure 4).

With these four catalysts in hand, their efficiencies were examined in the standard reaction between styrene and dimethyl α-diazobenzylphosphonate with 2,2-dimethylbutane (2,2-DMB) as the reaction solvent. In all cases, the cyclopropylphosphonate product **9** was generated in good-to-excellent yields (84–92%) and with levels of diastereoselectivity of $>$20:1 *E*/*Z* d.r.

In terms of enantioselectivity, the results indicate that the introduction of a substituent into the heterocyclic tether leads to a significant improvement in enantioselectivity. For example, [Rh_2(*S*-BPTTL)$_4$] generated the cyclopropane product with 86% *ee*, whereas the introduction of an extra phenyl group into the protecting group in [Rh_2(*S*-1-Ph-BPTTL)$_4$] (**5**) resulted in the generation of the product with 90% *ee* under the same reaction conditions (Table 1, entries 5 vs 7).

Moreover, the effect of introducing a *tert*-butyl group at the 4-position of the phthalimido group in [Rh_2(*S*-^{tert}PTTL)$_4$] was

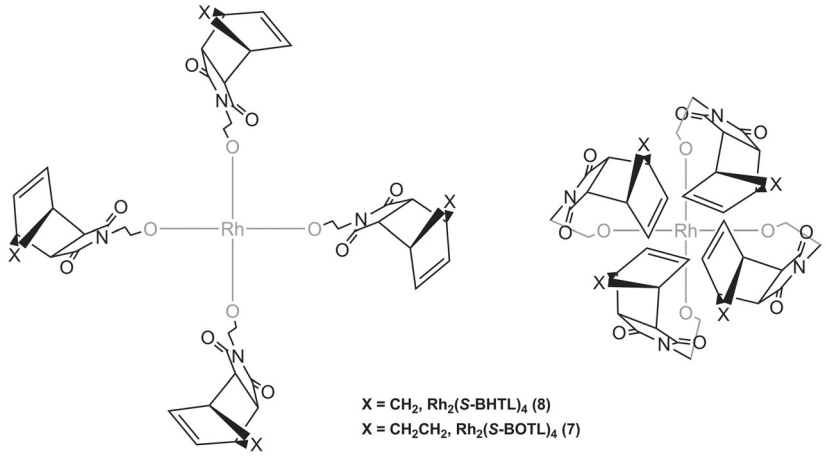

Figure 4. Two possible orientations for the N-protecting group in $[Rh_2(S\text{-BOTL})_4]$ (**7**) and $[Rh_2(S\text{-BHTL})_4]$ (**8**).

Table 1. Asymmetric cyclopropanation of styrene with dimethyl diazobenzylphosphonate (donor–acceptor substrate).[a]

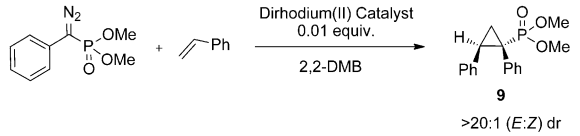

9

>20:1 (*E*:*Z*) dr

	Catalyst	Catalyst code	Reaction temp. [°C]	Yield [%]	*ee* [%]
1	$[Rh_2(S\text{-PTAD})_4]$	–	59	86	94
2	$[Rh_2(S\text{-PTAD})_4]$	–	23[b]	49	66
3	$[Rh_2(S\text{-PTTL})_4]$	–	59	85	92
4	$[Rh_2(S\text{-NTTL})_4]$	–	59	87	91
5	$[Rh_2(S\text{-BPTTL})_4]$	–	59	83	86
6	$[Rh_2(S\text{-1,2-NTTL})_4]$	–	59	93	92
7	$[Rh_2(S\text{-1-Ph-BPTTL})_4]$	**5**	59	87	90
8	$[Rh_2(S\text{-}^{tert}\text{PTTL})_4]$	**6**	23[b]	92	98
9	$[Rh_2(S\text{-BOTL})_4]$	**7**	59	89	66
10	$[Rh_2(S\text{-BHTL})_4]$	**8**	59	84	74

[a] Heated at reflux, unless stated otherwise, until TLC indicated complete consumption of the diazo starting material. Diastereomeric ratios (d.r.) were determined by ^{1}H NMR analysis of the crude reaction mixtures. Enantiomeric excesses (*ee*) were determined by chiral HPLC using a Chiralcel OJ column, 2% 2-propanol in *n*-hexane (v/v%), 1 mL min^{-1}, 220 nm, $t_1 = 18$ min, $t_2 = 21$ min. [b] Stirring overnight. [c] Stirring for 5 h.

dramatic. $[Rh_2(S\text{-}^{tert}\text{PTTL})_4]$ (**6**) is fully soluble in 2,2-DMB at room temperature and, generally, it provided improved levels of enantioinduction compared with $[Rh_2(S\text{-PTTL})_4]$ and $[Rh_2(S\text{-NTTL})_4]$ (Table 1, entries 8 vs 3 and 4). In the presence of $[Rh_2(S\text{-PTTL})_4]$ and $[Rh_2(S\text{-NTTL})_4]$, cyclopropane **9** was generated with 92 and 91% *ee*, respectively, whereas, after stirring for 5 h at room temperature, the $[Rh_2(S\text{-}^{tert}\text{PTTL})_4]$-catalysed reaction proceeded smoothly to generate the cyclopropane product **9** with 98% *ee* (Table 1, entry 8).

This result is superior to that obtained when $[Rh_2(S\text{-PTAD})_4]$ was used as catalyst in the same reaction carried out at reflux (59 °C) for 13 h.[4] The $[Rh_2(S\text{-PTAD})_4]$-catalysed cyclopropanation reaction performed with stirring at room temperature overnight gave the cyclopropane product in a yield of 49% with an enantioselectivity of 66% *ee* (Table 1, entry 2). At this point, and based on the results obtained, it was realised that a much more synthetically accessible alternative to $[Rh_2(S\text{-PTAD})_4]$ might have been discovered.

Unfortunately, the bicyclic complexes $[Rh_2(S\text{-BOTL})_4]$ (**7**) and $[Rh_2(S\text{-BHTL})_4]$ (**8**) did not return the expected success. The cyclopropanation reactions proceeded successfully giving the cyclopropane product with moderate enantioselectivities of 66 and 74% *ee*, respectively (Table 1, entries 9 and 10).

The carbenoid cyclopropanation reaction of dimethyl α-diazobenzylphosphonate was applied to a range of olefins using $[Rh_2(S\text{-1-Ph-BPTTL})_4]$ (**5**) and $[Rh_2(S\text{-}^{tert}\text{PTTL})_4]$ (**6**) as catalysts and the results are presented in Table 2. All the reactions involving $[Rh_2(S\text{-}^{tert}\text{PTTL})_4]$ (**6**) were carried out at room temperature, whereas the reactions involving $[Rh_2(S\text{-1-Ph-BPTTL})_4]$ (**5**) were carried out at 59 °C. In all cases, the reactions proceeded smoothly resulting in the formation of the corresponding cyclopropylphosphonate products in very high yields (82–93%) and diastereoselectivities (>20:1 *E*/*Z* d.r.). In terms of enantioselectivity, $[Rh_2(S\text{-}^{tert}\text{PTTL})_4]$ (**6**) was the best catalyst giving the corresponding cyclopropane products with very high levels of enantioselectivity (>98–99% *ee*).

Table 2. Scope of the catalysts with respect to the alkene.[a]

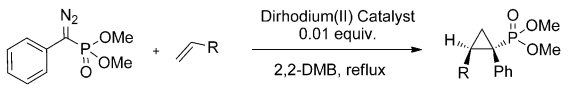

>20:1 (*E*:*Z*) dr

	R	Product	$[Rh_2(S\text{-1-Ph-BPTTL})_4]$ (**5**) Yield [%]	*ee* [%]	$[Rh_2(S\text{-}^{tert}\text{PTTL})_4]$[b] (**6**) Yield [%]	*ee* [%]
1	*p*-ClPh	**10**	89	84	94	>98
2	*p*-MeOPh	**11**	86	93	90	99
3	*p*-MePh	**12**	88	90	93	>99
4	1-naphthyl	**13**	82	90	85	>98

[a] Diastereomeric ratios (d.r.) were determined by ^{1}H NMR analysis of the crude reaction mixtures. Enantiomeric excesses (*ee*) were determined by chiral HPLC. See the Experimental Section for chromatographic conditions and details. [b] Stirring at room temperature.

The relative and absolute configuration of dimethyl 1-phenyl-2-(*p*-methylphenyl)cyclopropylphosphonate (**12**) was determined by X-ray crystallographic analysis to be (1*S*,2*R*), which is in agreement with the predicted assignment. The structures of all the other cyclopropylphosphonate derivatives were tentatively assigned the same relative and absolute configuration by analogy to **12** and based on the assumption that all reactions occur through similar transition states.

The effect of the size of the diazophosphonate ester groups on the enantioselectivity of the cyclopropanation reaction performed with catalysts **5** and **6** was next examined by using a series of diazophosphonate derivatives. The results are summarised in Table 3 and reveal that the diastereoselectivity is independent of the size of the phosphonate group and not greatly influenced by the size of the ester groups. However, in all cases, increasing the size of the ester group caused a drastic decrease in both the yield and enantioselectivity, with the highest yield and enantioselectivity observed with dimethyl α-diazobenzylphosphonate (Table 3, entry 1).

Crystallographic studies on $[Rh_2(S\text{-1-Ph-BPTTL})_4]$ (**5**), $[Rh_2(S\text{-}^{tert}PTTL)_4]$ (**6**), $[Rh_2(S\text{-BOTL})_4]$ (**7**) and $[Rh_2(S\text{-BHTL})_4]$ (**8**) were carried out to clarify the nature of the observed enhancement effect exhibited by lowering the symmetry of the N-protecting group on the enantioinduction.

In the published structure of the mono-EtOAc adduct of $[Rh_2(S\text{-PTTL})_4]$,[18] the flow of the ligand based chirality can be seen to give rise to a "chiral binding pocket" or "chiral crown cavity". The nature of the chirality of this binding pocket is based on two important features (Figure 5a): 1) the C_α–CO_2 single bond torsion (carboxylate carbon to α-carbon bond), which causes the C_α–N bond to twist clockwise towards the carbene binding pocket (when viewed along the Rh–Rh axis in the chiral cavity) and 2) the N–C_α bond torsion, which allows docking of the adjacent N-phthaloyl units featuring O···CH closest contacts. Figure 5b,c schematically depict the "daisy chain" manner in which the binding pocket is constructed.[16]

The X-ray crystal structures of both bis(ACN) and bis(THF) adducts of $[Rh_2(S\text{-}^{tert}PTTL)_4]$ (**6**) were obtained from samples recrystallised from acetonitrile and THF, respectively. Both

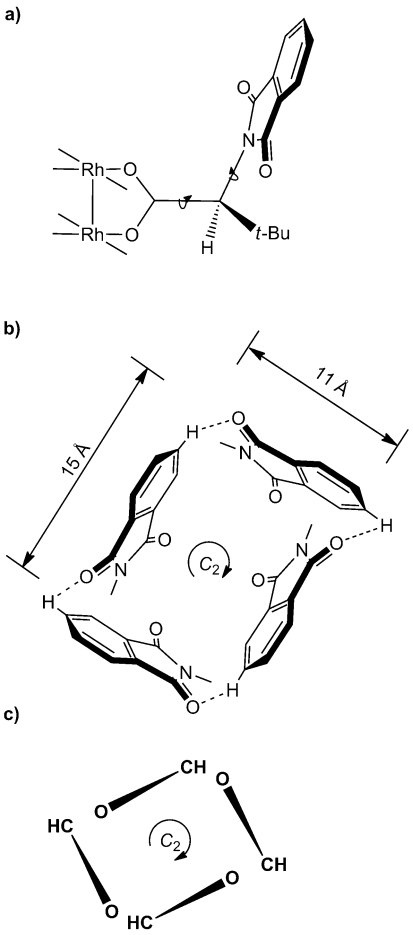

Figure 5. a) Features that determine the chirality to binding pocket of $[Rh_2(S\text{-PTTL})_4]$ and its analogues. b,c) Schematic illustration of the "daisy-chain" manner in which the rectangular binding pocket of $[Rh_2(S\text{-PTTL})_4]$ is constructed.

adducts reveal a chiral crown conformation in which all four N-protecting groups are equivalently positioned around the extremity of the chiral crown cavity without reducing the C_4 symmetry of the catalyst (Figure 6). The *tert*-butyl substituents are similarly disposed towards the "corner" of the square-shaped cavity. The chiral cavity is rigorously C_4-symmetrical in the solid state (in both the bis(ACN) and bis(THF) adducts), whereas the four N-(4-*tert*-butylphthaloyl) groups maintain the chiral nature of the crown cavity surrounding the axial rhodium coordination site through the clockwise twist of these groups.

The square cavity of $[Rh_2(S\text{-}^{tert}PTTL)_4]$ (**6**) contrasts with the rectangular conformer originally reported for the mono-EtOAc adduct of $[Rh_2(S\text{-PTTL})_4]$ (Figure 7).[18] The additional substitution on the N-phthaloyl group in $[Rh_2(S\text{-}^{tert}PTTL)_4]$ can be seen to extend the width of each of the cavity walls to the point that adjacent ligands are nearly in van der Waals contact. Furthermore, from a comparison of the space-filling representations of $[Rh_2(S\text{-}^{tert}PTTL)_4]$ and $[Rh_2(S\text{-PTTL})_4]$, it is clear that the extra *tert*-butyl substituents in $[Rh_2(S\text{-}^{tert}PTTL)_4]$ lead to greater ligand conformational rigidity through C_α–CO_2 and N–C_α bond torsions of the ligands. On the other hand, this is not the case for the unsubstituted $[Rh_2(S\text{-PTTL})_4]$ and various other contort-

Table 3. Effect of the size of the α-diazophosphonate ester groups on the enantioselectivity of the catalysts.[a]

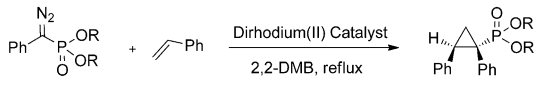

	R	Product	$[Rh_2(S\text{-1-Ph-BPTTL})_4]$ (**5**) Yield [%]	*ee* [%]	$[Rh_2(S\text{-}^{tert}PTTL)_4]$[b] (**6**) Yield [%]	*ee* [%]
1	Me	**9**	87	92	92	99
2	Et	**14**	66	54	74	92
3	*i*Pr	**15**	38	48[c]	40	64[c]

[a] Diastereomeric ratios (d.r.) were determined by ^{1}H NMR analysis of the crude reaction mixtures. Enantiomeric excesses (*ee*) were determined by chiral HPLC. See the Experimental Section for chromatographic conditions and details. [b] Stirring at room temperature. [c] Heated at reflux for 3 days.

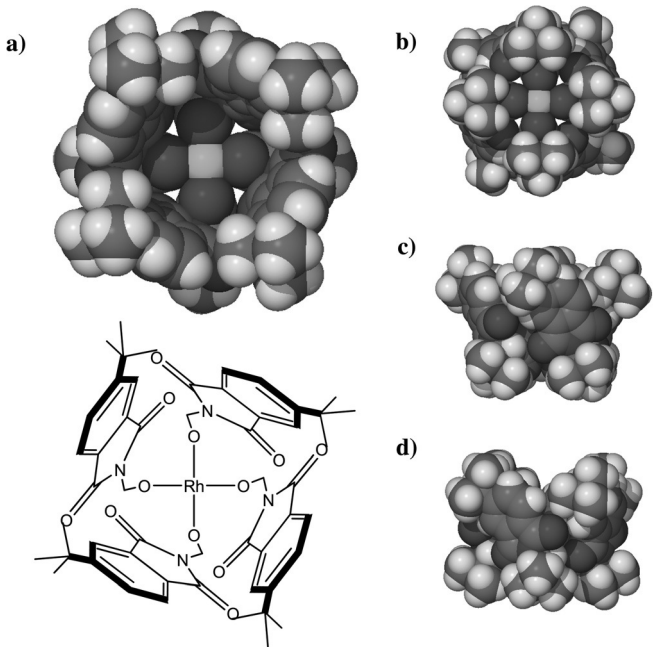

Figure 6. Molecular structure of the bis(THF) adduct of $[Rh_2(S\text{-}^{tert}PTTL)_4]$ (**6**). Space-filling representations: a) top view, b) bottom view and c,d) side views. A second similar molecule as well as axial ligands have been omitted for clarity.

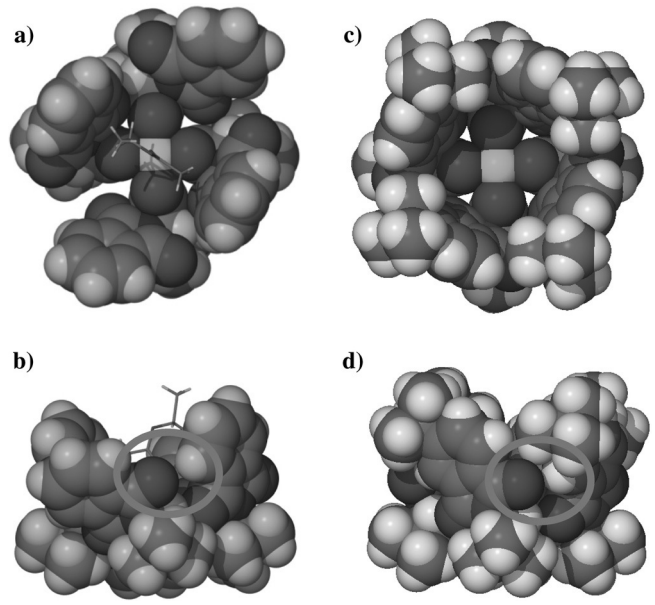

Figure 7. Space-filling structure comparison of the EtOAc adduct of $[Rh_2(S\text{-PTTL})_4]$ and the bis(THF) adduct of $[Rh_2(S\text{-}^{tert}PTTL)_4]$ (**6**). a,c) Top views of $[Rh_2(S\text{-PTTL})_4]$ and $[Rh_2(S\text{-}^{tert}PTTL)_4]$, respectively, b,d) side views of $[Rh_2(S\text{-PTTL})_4]$ and $[Rh_2(S\text{-}^{tert}PTTL)_4]$, respectively.

ed chiral cavities that have been crystallographically observed.[13b,16,18] The gaps at the corners of these cavities allow substantial variation around the C_α–CO_2 and N–C_α bond torsions. Therefore, the additional *tert*-butyl substitution in $[Rh_2(S\text{-}^{tert}PTTL)_4]$ relieves the overall chiral twist of the cavity without introducing additional steric hindrance at the axial positions. Therefore, if this geometry is also relevant to the solution structures adopted during catalysis, it may be linked to the observed enhanced enantioinduction relative to the parent catalyst $[Rh_2(S\text{-PTTL})_4]$.

For a superior understanding of the enhanced selectivity, the structure obtained for $[Rh_2(S\text{-}^{tert}PTTL)_4]$ was also compared with the X-ray structure of $[Rh_2(S\text{-PTAD})_4]$. The X-ray structure of the former resembles to a large extent the X-ray crystal structure of the latter catalyst (Figure 8). $[Rh_2(S\text{-PTAD})_4]$ was observed to form a bis(EtOAc) adduct with an $\alpha,\alpha,\alpha,\alpha$ conformation in the solid state when crystallised from an ethyl acetate/*n*-hexane solvent mixture. All four N-phthaloyl protecting groups sit evenly around the edge of a fairly square cavity to afford a C_4-symmetric catalyst molecule (Figure 8). The width across the cavity faces was found to be between 14.1 and 16.0 Å. From the space-filling representation of $[Rh_2(S\text{-PTAD})_4]$, it can be anticipated that the bulkier adamantyl groups introduce a greater conformational rigidity through only C_α–CO_2 bond torsions of the ligands, whereas the N–C_α bond torsions remain flexible. Therefore, $[Rh_2(S\text{-PTAD})_4]$ is expected to have a more rigid chiral cavity than its parent $[Rh_2(S\text{-PTTL})_4]$, but less rigid than $[Rh_2(S\text{-}^{tert}PTTL)_4]$ (**6**). In addition, $[Rh_2(S\text{-PTAD})_4]$ retains the same gaps at the corners of the chiral cavity as found in $[Rh_2(S\text{-PTTL})_4]$.

Another important feature to note is that the crystal structure of $[Rh_2(S\text{-PTAD})_4]$ has an ethyl acetate molecule coordinated to each rhodium centre, which confirms that there is still enough room for a Lewis basic ligand to coordinate to the "achiral" axial rhodium coordination site (the site shrouded by adamantyl substituents). This observation confirms that both

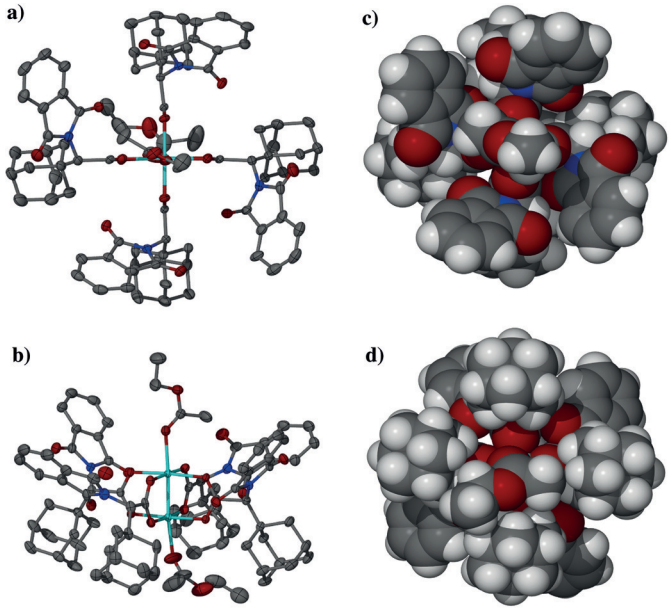

Figure 8. Molecular structure of the bis(EtOAc) adduct of $[Rh_2(S\text{-PTAD})_4]$ a) viewed from above the chiral crown cavity and b) general view. All hydrogen atoms, a second similar molecule and lattice solvent have been omitted for clarity. Space-filling representations viewed along the Rh–Rh axis c) from above the chiral crown cavity d) onto the axial rhodium coordination site shrouded by the adamantyl groups.

rhodium atoms are still accessible to the diazo substrates, even after the introduction of the more bulky adamantyl groups. This observation contrasts with the hypothesis of Fox and co-workers[18] in relation to the full chiral crown conformer in the Hashimoto-type dirhodium catalysts and the foundation for the development of the $[Rh_2(S\text{-PTAD})_4]$ catalyst.[4]

The X-ray crystal structure of the bis(EtOAc) adduct of $[Rh_2(S\text{-1-Ph-BPTTL})_4]$ (**5**; Figure 9) was also determined and shows that the complex also adopts the α,α,α,α conformation in the solid state with all four N-protected amino acid ligands being directed towards the same axial coordination site of the C_4-symmetric chiral paddlewheel complex. The molecule exhibits a perfectly regular cavity, with each of the four aryl units comprising the cavity walls having a clockwise twisted arrangement with a cavity width of 13.4 Å between opposite faces. Although retaining the same clockwise twist, the phenyl substituents point towards the opposite side of the protecting group rings compared with the *tert*-butyl substituents in $[Rh_2(S\text{-}^{tert}\text{PTTL})_4]$ (**6**). The substituents are ordered with respect to the C_4 axis of the catalyst. This again widens the walls of the cavity relative to its parent $[Rh_2(S\text{-BPTTL})_4]$[16] structure creating significantly smaller gaps at the corners of the cavity and significantly less variation in the C_α–CO_2 and N–C_α bond rotations.

The X-ray crystal structures of $[Rh_2(S\text{-BOTL})_4]$ (**7**) and $[Rh_2(S\text{-BHTL})_4]$ (**8**) were also obtained; both revealed crown structures, as described above for $[Rh_2(S\text{-PTTL})_4]$, $[Rh_2(S\text{-PTAD})_4]$, $[Rh_2(S\text{-}^{tert}\text{PTTL})_4]$ and $[Rh_2(S\text{-1-Ph-BPTTL})_4]$. The N-protecting groups in $[Rh_2(S\text{-BHTL})_4]$ (**8**) are all directed in the same way with the *syn*-annulated cyclopentene extremities pointing into the cavity

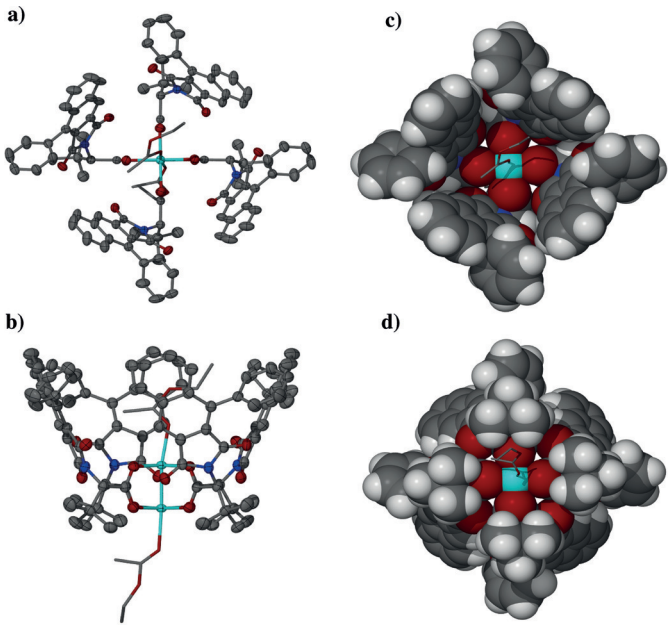

Figure 9. Molecular structures of the bis(EtOAc) adduct of $[Rh_2(S\text{-1-Ph-BPTTL})_4]$ (**5**) a) viewed along the axis of the chiral crown cavity and b) side view. All hydrogen atoms, a second similar molecule and lattice solvent have been omitted for clarity. Space-filling representations viewed along the Rh–Rh axis c) from above the chiral crown cavity, d) onto the axial rhodium coordination site shrouded by the *tert*-butyl groups.

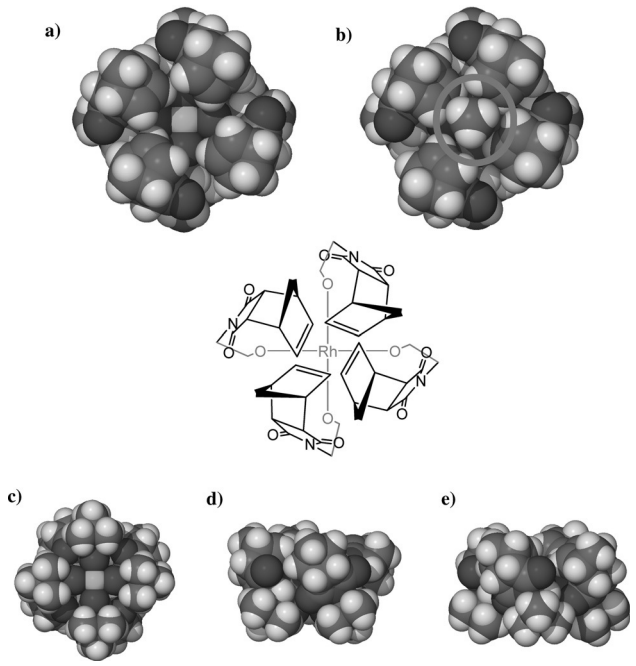

Figure 10. Molecular structure of the bis(ACN) adduct of $[Rh_2(S\text{-BHTL})_4]$ (**8**). Space-filling representations (ACN removed except in b): a) top view, b) prolate-shaped ACN axial ligand entirely shrouded by cavity walls, c) bottom view and d,e) side views.

and the axially bonded prolate-shaped ACN ligand entirely shrouded by the cavity walls (Figure 10). This does not reduce the overall higher-order chirality of the complex as each ligand is similarly disposed and the ligand extremities contribute to the overall C_4 symmetry of the chiral cavity. The top of the cavity is "square" and it is very congested for the binding of substrates during catalysis, apparent in the space-filling representation of the complex (Figure 10a,b). For this catalyst to be functional, it is anticipated that some of the N-protecting groups need to rotate (flip with respect to N–C_α bond rotation) and/or lose the crown conformation to provide enough room for the binding of larger substrates (Figure 4). Otherwise, the crown cavity will remain too crowded for the substrate to bind and possibly lead to the other "achiral" rhodium centre competing to play a greater role. If the latter is the case, this could justify the observed relatively low enantioselectivity of **8**.

The X-ray structure of $[Rh_2(S\text{-BOTL})_4]$ (**7**) reveals an α,α,α,α crown conformer with one ligand orientated differently to that normally seen in other α,α,α,α analogues and with all four amino acid derived ligands maintaining their *S*-stereogenic carbon centres (Figure 11). The examination of several crystals indicated the same morphology. This is in contrast to the clockwise twist observed for $[Rh_2(S\text{-BHTL})_4]$ (**8**) discussed above. For $[Rh_2(S\text{-BOTL})_4]$ (**7**) crystallised from MeOH, the positioning of the non-rhodium-bound MeOH lattice molecule, which forms hydrogen bonds with the MeOH bonded to the rhodium in the chiral cavity, is influential. In the catalyst, one of the *S*-BOTL ligands is forced, unusually, to shift to create room for the hydrogen-bonded MeOH molecule (Figure 11a,b). It is also important to highlight that the extremities of the N-

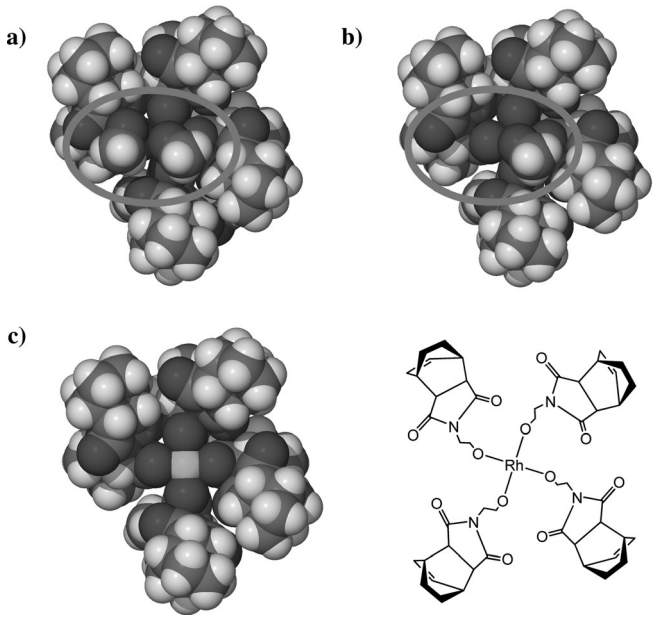

Figure 11. Molecular structures of the bis(MeOH) adduct of $[Rh_2(S\text{-BOTL})_4]$ (**7**). Space-filling structures: a,b,c) three pictures of the complex in various states of "undressing" of the MeOH ligands around the cavity.

Table 4. Asymmetric cyclopropanation of styrene with 2,2,2-triflurometh-yl-1-phenyldiazoethane (donor–acceptor substrate).[a]

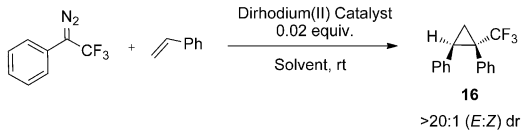

16

>20:1 (*E*:*Z*) dr

	Catalyst	Catalyst code	Solvent	Yield [%]	*ee* [%]
1	$[Rh_2(S\text{-PTAD})_4]$	–	TFT	95	88
2	$[Rh_2(S\text{-PTTL})_4]$	–	TFT	96	82
3	$[Rh_2(S\text{-NTTL})_4]$	–	TFT	95	79
4	$[Rh_2(S\text{-4-Br-NTTL})_4]$	–	TFT	83	78
5	$[Rh_2(S\text{-1,2-NTTL})_4]$	–	TFT	85	82
6	$[Rh_2(S\text{-1-Ph-BPTTL})_4]$	**5**	TFT	69	42
7	$[Rh_2(S\text{-}^{tert}\text{PTTL})_4]$	**6**	TFT	99	88
8	$[Rh_2(S\text{-}^{tert}\text{PTTL})_4]$	**6**	2,2-DMB	97	88

[a] Diastereomeric ratios (d.r.) were determined by ^{1}H NMR analysis of the crude reaction mixtures. Enantiomeric excesses (*ee*) were determined by chiral HPLC using a Chiralcel OJ column, 1% 2-propanol in *n*-hexane (v/v%), 0.8 mL min^{-1}, 220 nm, $t_1 = 5.5$ min, $t_2 = 6.8$ min.

protecting group do not face in towards the top of the cavity but outwards, which is opposite to the related complex **8** described above.

The structural features of complexes **7** and **8** are very important as they strongly indicate that these two complexes lack the conformational rigidity through both C_α–CO_2 and N–C_α bond torsions of the ligands. It can be speculated that the flexibility of the ligands in both $[Rh_2(S\text{-BOTL})_4]$ (**7**) and $[Rh_2(S\text{-BHTL})_4]$ (**8**) could have led to irregular cavities similar to that observed in **7** when substrates binds to it. This, in turn, may lead to different selectivities, accounting for the relatively low enantioselectivities observed in the reactions with these complexes.

More extensive structural investigations need to be undertaken before any generalities should be drawn regarding the effects of axial-bound ligands on the conformational preference of this class of complexes.

The scope of the new catalysts was also investigated by studying cyclopropanation reactions involving donor–acceptor carbenoid intermediates containing CF_3 as an electron-withdrawing group using the reported optimised reaction conditions.[7] The fluoro functionality impacts profoundly on the chemical, physical and biological properties of organic compounds[19] and is generally used to tune the pharmacokinetic, electronic,[20] steric[21] and lipophilic[22] properties of different pharmaceutical agents.

The results summarised in Table 4 reveal a similar enhancement in enantioselectivity for the cyclopropanation of styrene with 2,2,2-trifluromethyl-1-phenyldiazoethane. Generally, the product **16** was generated in high yields and with high levels of diastereoselectivity (>20:1 *E*/*Z* d.r.) by using α,α,α-trifluorotoluene (TFT) as solvent.

With respect to enantioselectivity, the results show that the product was generated in 88% *ee* with $[Rh_2(S\text{-}^{tert}\text{PTTL})_4]$ (**6**) as catalyst (Table 4, entry 7), and that changing the reaction solvent to 2,2-DMB did not impact on its enantioselectivity (Table 4, entry 8). The enantioselectivity observed with $[Rh_2(S\text{-}^{tert}\text{PTTL})_4]$ was analogous to that observed when $[Rh_2(S\text{-PTAD})_4]$ was applied in the same reaction under the same reaction conditions (Table 4, entry 1) whereas in the $[Rh_2(S\text{-PTTL})_4]$-, $[Rh_2(S\text{-NTTL})_4]$- and $[Rh_2(S\text{-1,2-NTTL})_4]$-catalysed reactions, the cyclopropane product **16** was generated in lower enantioselectivities of 82, 79 and 82% *ee*, respectively. $[Rh_2(S\text{-1-Ph-BPTTL})_4]$ (**5**) was found to be unsuitable for this reaction, generating the cyclopropane in 42% *ee*. The relative and absolute stereochemistry of the product was again unambiguously assigned to be (1*S*,2*R*) by means of X-ray crystallography analysis.

The next series of experiments were carried out on diazoacetates as another example of donor–acceptor diazo-substrates. The new catalysts were evaluated in the cyclopropanation reaction of styrene with methyl *p*-methoxyphenyldiazoacetate, which generates methyl 1,2-diphenylcyclopropanecarboxylate **17**; the results are summarised in Table 5. All the catalysts afforded the cyclopropane product **17** with excellent diastereoselectivity (>18:1 *E*/*Z* d.r.).

Considering the enantioselectivity of the reaction, generally, the results reveal that $[Rh_2(S\text{-}^{tert}\text{PTTL})_4]$ (**6**) is a better catalyst than $[Rh_2(S\text{-PTAD})_4]$ at a catalyst loading of 0.01 equivalents and similar to $[Rh_2(S\text{-PTTL})_4]$. In contrast, $[Rh_2(S\text{-1-Ph-BPTTL})_4]$ (**5**) and $[Rh_2(S\text{-NTTL})_4]$ are totally incompatible with this class of substrate with quite poor enantioselectivities (10 and 42% *ee*, respectively). Increasing the $[Rh_2(S\text{-}^{tert}\text{PTTL})_4]$ (**6**) catalyst loading from 0.01 to 0.05 equivalents had a minimal effect on both yield and enantioselectivity (Table 5, entries 7 and 8). Furthermore, changing the reaction solvent to 2,2-DMB slightly enhanced the enantioselectivity of $[Rh_2(S\text{-}^{tert}\text{PTTL})_4]$ (**6**) to 78% *ee* (Table 5, entries 7 and 9).

Table 5. Asymmetric cyclopropanation of styrene with methyl *p*-methoxyphenyldiazoacetate (donor–acceptor substrate).[a]

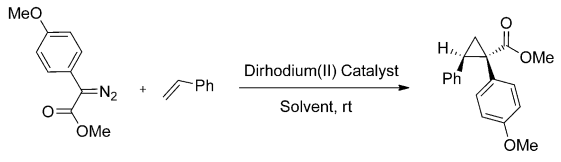

17

>18:1 (*E*:*Z*) dr

	Catalyst	Catalyst code	Solvent	Catalyst loading [equiv]	Yield [%]	*ee* [%]
1	$[Rh_2(S\text{-PTAD})_4]$	–	pentane	0.01	96	73
2	$[Rh_2(S\text{-PTTL})_4]$	–	pentane	0.01	84	78
3	$[Rh_2(S\text{-NTTL})_4]$	–	pentane	0.01	83	42
4	$[Rh_2(S\text{-1,2-NTTL})_4]$	–	pentane	0.01	84	70
5	$[Rh_2(S\text{-1-Ph-BPTTL})_4]$	**5**	pentane	0.01	80	8
6	$[Rh_2(S\text{-1-Ph-BPTTL})_4]$	**5**	2,2-DMB	0.01	83	10
7	$[Rh_2(S\text{-}^{tert}\text{PTTL})_4]$	**6**	pentane	0.01	80	76
8	$[Rh_2(S\text{-}^{tert}\text{PTTL})_4]$	**6**	pentane	0.05	83	76
9	$[Rh_2(S\text{-}^{tert}\text{PTTL})_4]$	**6**	2,2-DMB	0.01	85	78

[a] Diastereomeric ratios (d.r.) were determined by ^{1}H NMR analysis of the crude reaction mixtures. Enantiomeric excesses (*ee*) were determined by chiral HPLC using a Chiralcel® OD-H column, 0.7% 2-propanol in *n*-hexane (v/v%), 1 mL min^{-1}, 220 nm, $\tau_1 = 13$ min, $\tau_2 = 23$ min.

Table 6. Asymmetric cyclopropanation of styrene with α-phenyldiazoacetate (donor–acceptor substrate).[a]

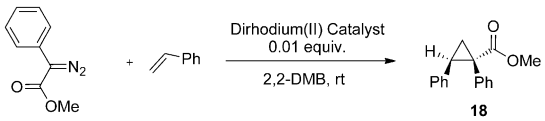

18

>18:1 (*E*:*Z*) dr

	Catalyst	Catalyst code	Yield [%]	*ee* [%]
1	$[Rh_2(S\text{-PTAD})_4]$[5]	–	87	21[b]
2	$[Rh_2(S\text{-PTTL})_4]$	–	87	20
3	$[Rh_2(S\text{-NTTL})_4]$	–	88	8
4	$[Rh_2(S\text{-1-Ph-BPTTL})_4]$	**5**	90	30[c]
5	$[Rh_2(S\text{-}^{tert}\text{PTTL})_4]$	**6**	87	46
6	$[Rh_2(S\text{-1,2-NTTL})_4]$	–	89	30
7	$[Rh_2(S\text{-BOTL})_4]$	**7**	66	38
8	$[Rh_2(S\text{-BHTL})_4]$	**8**	58	17

[a] Diastereomeric ratios (d.r.) were determined by ^{1}H NMR analysis of the crude reaction mixtures. Enantiomeric excesses (*ee*) were determined by chiral HPLC using a Chiralcel OJ column, 1% 2-propanol in *n*-hexane (v/v%), 0.8 mL min^{-1}, 220 nm, $t_1 = 5.5$ min, $t_2 = 6.8$ min. [b] In toluene. [c] The opposite enantiomer was observed.

Table 7. Asymmetric cyclopropanation of styrene with methyl 2-diazo-4-phenylbut-3-enoate (donor–acceptor substrate).[a]

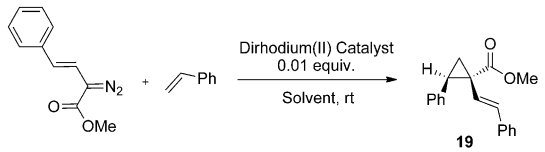

19

>18:1 (*E*:*Z*) dr

	Catalyst	Catalyst code	Solvent	Yield [%]	*ee* [%]
1	$[Rh_2(S\text{-PTTL})_4]$	–	CH_2Cl_2	83	40
2	$[Rh_2(S\text{-NTTL})_4]$	–	CH_2Cl_2	82	16
3	$[Rh_2(S\text{-1-Ph-BPTTL})_4]$	**5**	2,2-DMB	86	19[b]
4	$[Rh_2(S\text{-}^{tert}\text{PTTL})_4]$	**6**	2,2-DMB	86	44
5	$[Rh_2(S\text{-1,2-NTTL})_4]$	–	CH_2Cl_2	88	10
6	$[Rh_2(S\text{-1,2-NTTL})_4]$	–	pentane	87	10
7	$[Rh_2(S\text{-BOTL})_4]$	**7**	pentane	69	4
8	$[Rh_2(S\text{-BHTL})_4]$	**8**	2,2-DMB	77	2

[a] Diastereomeric ratios (d.r.) were determined by ^{1}H NMR analysis of the crude reaction mixtures. Enantiomeric excesses (*ee*) were determined by chiral HPLC using a Chiralcel OJ column, 1.5% 2-propanol in *n*-hexane (v/v%), 1 mL min^{-1}, 254 nm, $t_1 = 15$ min, $t_2 = 21$ min. [b] The opposite enantiomer was observed.

Catalyst screening was further extended by removing the *p*-methoxy group from the diazoacetate. The cyclopropanation reaction of styrene with methyl 2-diazo-2-phenylacetate was carried out with a catalyst loading of 0.01 equivalents. As illustrated in Table 6, all the catalysts afforded the cyclopropane product **18** in good-to-excellent yields (65–89%) and with high diastereoselectivities (>18:1 *E*/*Z* d.r.). However, the asymmetric induction was dramatically reduced upon removal of the *p*-methoxy group. The best enantiomeric induction was 46% *ee* with $[Rh_2(S\text{-}^{tert}\text{PTTL})_4]$ (**6**; Table 6, entry 5).

It is important to note that although $[Rh_2(S\text{-1-Ph-BPTTL})_4]$ (**5**) is derived from protected L-*tert*-leucine, like the rest of complexes screened, its use in this reaction resulted in the formation of the corresponding cyclopropane product **18** in 30% *ee*, but with the opposite absolute configuration (Table 6, entry 4). This may be related to the opposite alignment of the phenyl substituents on the N-protecting group rings. Further investigations are still required regarding this point.

A series of experiments were also carried out with methyl (*E*)-2-diazo-4-phenylbut-3-enoate (Table 7). In all cases, excellent levels of diastereoselectivity were observed, however, the best enantiomeric induction was 44% *ee* when $[Rh_2(S\text{-}^{tert}\text{PTTL})_4]$ (**6**) was used as the catalyst (Table 7, entry 4). Similar behaviour to that discussed above was witnessed with $[Rh_2(S\text{-1-Ph-BPTTL})_4]$ (**5**); this catalyst gave the cyclopropane product **19** in 19% *ee*, but with the opposite absolute configuration (Table 7, entry 3).

The scope of the new catalysts was further investigated by performing cyclopropanation reactions involving donor–acceptor carbenoid intermediates containing CN as an electron-withdrawing group using the optimised reaction conditions reported by Davies and co-workers.[6] The results are illustrated in Table 8.

The cyclopropane product **20** was generated in high yields for all catalysts. In terms of diastereoselectivity, although $[Rh_2(S\text{-PTTL})_4]$ and $[Rh_2(S\text{-}^{tert}\text{PTTL})_4]$ (**6**) offered an acceptable diastereoselectivity of >20:1 (*E*/*Z*) d.r., $[Rh_2(S\text{-PTAD})_4]$ was the best among the screened complexes with a diastereomeric ratio of 64:1 (*E*/*Z*). The diastereoselectivity of the cyclopropane product generated by $[Rh_2(S\text{-1,2-NTTL})_4]$ did not exceed 11:1 (*E*/*Z*) d.r.. This system has been studied previously and it was proposed that the variable diastereoselectivity observed was due to the small size of the nitrile acceptor group.[6]

Table 8. Asymmetric cyclopropanation of styrene with α-phenyl-α-diazoacetonitrile (donor–acceptor substrate).[a]

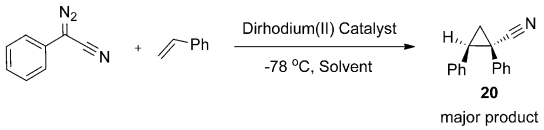

	Catalyst	Catalyst code	Catalyst loading [equiv]	Solvent	Yield [%][b]	d.r. (*E*/*Z*)	*ee* [%]	
							Major diastereomer	Minor diastereomer
1	$[Rh_2(OAc)_4]$	–	0.02	toluene	82	4:1[c]	–	–
2	$[Rh_2(S\text{-PTAD})_4]$	–	0.02	toluene	85	64:1	80	74
3	$[Rh_2(S\text{-PTTL})_4]$	–	0.02	toluene	84	27:1	86	78
4	$[Rh_2(S\text{-NTTL})_4]$	–	0.02	toluene	84	13:1	90	92
5	$[Rh_2(S\text{-1,2-NTTL})_4]$	–	0.02	toluene	80	11:1	83	76
6	$[Rh_2(S\text{-1-Ph-BPTTL})_4]$	**5**	0.02	toluene	84	7:1	30	78
7	$[Rh_2(S\text{-}^{tert}\text{PTTL})_4]$	**6**	0.02	toluene	83	25:1	82	84
8	$[Rh_2(S\text{-}^{tert}\text{PTTL})_4]$	**6**	0.01	toluene	81	26:1	82	86
9	$[Rh_2(S\text{-}^{tert}\text{PTTL})_4]$	**6**	0.02	2,2-DMB	83	16:1	82	82

[a] Diastereomeric ratios (d.r.) were determined by ^{1}H NMR analysis of the crude reaction mixtures. Enantiomeric excesses (*ee*) were determined by chiral HPLC using a Chiralcel OD column, 0.8% 2-propanol in *n*-hexane (v/v%), 1 mL min^{-1}, 220 nm, $t_1 = 19$ min, $t_2 = 29$ min. [b] Yield for both diastereomers. [c] Carried out at room temperature.

With regards to enantioselectivity, $[Rh_2(S\text{-}^{tert}\text{PTTL})_4]$ (**6**), $[Rh_2(S\text{-1,2-NTTL})_4]$, $[Rh_2(S\text{-PTTL})_4]$ and $[Rh_2(S\text{-PTAD})_4]$ revealed comparable enantioselectivity for the major diastereomer (80–86% *ee*). Erosion of neither the diastereo- nor enantioselectivity was observed when the $[Rh_2(S\text{-}^{tert}\text{PTTL})_4]$ loading was reduced from 0.02 to 0.01 equivalents. Also, changing the reaction solvent to 2,2-DMB did not affect the enantioselectivity of the major diastereomer, however, the diastereoselectivity was reduced to 16:1 (*E*/*Z*) d.r..

Regardless of its relatively low diastereoselectivity, $[Rh_2(S\text{-NTTL})_4]$ was the best catalyst in terms of enantioselectivity for this catalytic system. The catalyst gave the major and minor diastereomers of the cyclopropane products with enantiomeric excesses of 90 and 92%, respectively. On the other hand, $[Rh_2(S\text{-1-Ph-BPTTL})_4]$ (**5**) was completely incompatible with this reaction; the cyclopropane product was generated with a 7:1 (*E*/*Z*) d.r. and with 30% *ee* for the major diastereomer (Table 8, entry 6).

Conclusions

In this work a series of dirhodium(II) tetracarboxylates derived from (*S*)-amino acid ligands were prepared. A number of different approaches were explored to reduce the local symmetry of the ligand's heterocyclic tether. Four dirhodium(II) complexes were then prepared from these ligands, of which $[Rh_2(S\text{-}^{tert}\text{PTTL})_4]$ (**6**) proved to be an exceptional catalyst with extraordinary enantioselectivity (up to 99% *ee*). Screening of a number of different donor–acceptor diazo systems revealed that, generally, $[Rh_2(S\text{-}^{tert}\text{PTTL})_4]$ (**6**) is a much more enantioselective catalyst than $[Rh_2(S\text{-PTTL})_4]$ and $[Rh_2(S\text{-NTTL})_4]$, with a comparable enantioselectivity to $[Rh_2(S\text{-PTAD})_4]$. This is in addition to overcoming the synthetic limitations associated with $[Rh_2(S\text{-PTAD})_4]$ as it is much more synthetically accessible; $[Rh_2(S\text{-}^{tert}\text{PTTL})_4]$ (**6**) was prepared in high yield by a two-step procedure, whereas $[Rh_2(S\text{-PTAD})_4]$ is reported to have been prepared in more than 13 steps and takes around 2 weeks. In the synthesis of the cyclopropylphosphonate derivatives, $[Rh_2(S\text{-}^{tert}\text{PTTL})_4]$ (**6**) proved to offer an extra advantage over $[Rh_2(S\text{-PTAD})_4]$; $[Rh_2(S\text{-}^{tert}\text{PTTL})_4]$ (**6**) generated the corresponding cyclopropane products in high yields, diastereoselectivities and enantioselectivities after stirring at room temperature for 5 h, whereas similar reactions catalysed by $[Rh_2(S\text{-PTAD})_4]$ were performed at reflux over 10 h.[4] Our results have also demonstrated that $[Rh_2(S\text{-}^{tert}\text{PTTL})_4]$ (**6**) is compatible with some donor–acceptor diazoacetate substrates. This reflects its ability to complement the currently known flagship catalyst $[Rh_2(S\text{-DOSP})_4]$ and broadens the range of available catalysts for the asymmetric synthesis of chiral cyclopropanecarboxylate derivatives.

X-ray crystallography studies revealed that the structures of $[Rh_2(S\text{-}^{tert}\text{PTTL})_4]$ (**6**) and $[Rh_2(S\text{-PTAD})_4]$ are different to the X-ray crystal structure of $[Rh_2(S\text{-PTTL})_4]$ determined by Fox and co-workers, who suggested that $[Rh_2(S\text{-PTTL})_4]$ and related complexes are in a C_2-symmetric arrangement in the solid state.[18,23] From the comparison of the solid-state structures, it is evident that the extra *tert*-butyl groups introduced into $[Rh_2(S\text{-}^{tert}\text{PTTL})_4]$ (**6**) generate similar structural effects to the adamantyl groups in $[Rh_2(S\text{-PTAD})_4]$ as a result of the increase in the size of the substituents at the α positions. This was further confirmed by the comparable enantioselectivity observed for $[Rh_2(S\text{-}^{tert}\text{PTTL})_4]$ (**6**) and $[Rh_2(S\text{-PTAD})_4]$. Through the study of the halogen bond rigidification effect observed in chlorinated complexes, Charette and co-workers[12,24] highlighted the effect of chiral cavity rigidity on the enhancement of enantioselectivity. Herein, and based on the enantioselectivities achieved along with crystallographic observations of the new catalytic systems, it can be confirmed that the partial substitution of the ligand's N-heterocyclic tether is another factor towards reinforcing the rigidity of the cavity and enhancing the catalyst stereoselectivity.

It is also tempting to infer that the binding of identical MeOH axial ligands to each rhodium centre in $[Rh_2(S\text{-BOTL})_4]$ (**7**) does not result in a major α,α,α,α to α,α,β,β or α,β,α,β conformational flip. However, the C_4 symmetry of the chiral cavity was lost although the α,α,α,α conformation of the catalyst still exists.

All in all, and in the light of the results achieved, it is strongly believed that the "reduction of symmetry" approach developed here is an excellent new way to enhance the enantioselectivity of asymmetric dirhodium(II)-catalysed transformations. Further explorations related to this new trend are crucial to further confirm the impact of the lowering of local symmetry of the N-protecting group on the final enantioselectivity of the catalyst.

Experimental Section

Chemicals

All starting materials and reagents were purchased from Sigma–Aldrich, Acros Organics and Tokyo Chemical Industry Co. (TCI) and used without any further purification. All solvents were HPLC-grade and solvents used in dirhodium(II) carbenoid reactions were dried, distilled and degassed immediately prior to use: DCM over calcium hydride, *n*-pentane and toluene over sodium wire and chlorobenzene over potassium hydroxide. Anhydrous 2,2-DMB, TFT and THF were purchased from Sigma–Aldrich and degassed prior to use. All reactions were performed using oven-dried glassware and were flame-dried under vacuum prior to use. TLC was performed by using Sigma–Aldrich pre-coated silica gel 60 F254 aluminium supports (20×20 cm, 0.2 mm layer thickness) and spots were visualised by UV light (254 nm) or by using either 10% $KMNO_4$ or phosphomolybdic acid (PMA) as visualising agents. Preparative TLC purification was performed by using Sigma–Aldrich pre-coated silica gel 60 F254 glass supports (20×20 cm, 0.25 mm layer thickness). Column chromatography was carried out on silica gel 60 (130–270 mesh ASTM, Sigma–Aldrich) using the specified eluent compositions. The $[Rh_2(S\text{-PTTL})_4]$,[25] $[Rh_2(S\text{-NTTL})_4]$,[14] $[Rh_2(S\text{-BPTTL})_4]$,[26] and $[Rh_2(S\text{-1,2-NTTL})_4]$[15] catalysts were prepared according to reported procedures. $[Rh_2(OAc)_4]$ and $[Rh_2(S\text{-PTAD})_4]$ were purchased from Strem Chemicals.

Instruments

Melting points were measured on a Stuart-SMP10 melting point apparatus and are uncorrected. Optical rotations were measured by using a Perkin–Elmer 341 polarimeter at the sodium D line (589 nm) and are reported as $[\alpha]_D^{25}$ in g/100 mL concentration (*c*) in the solvents indicated. IR spectra were recorded on a Perkin–Elmer TravelIR FT-IR spectrometer. NMR spectra were recorded on Varian 400-MR and Varian Inova-500 spectrometers at room temperature in the solvents given. Chemical shifts are expressed in parts per million (ppm) and reported either relative to an internal tetramethylsilane standard (TMS: $\delta = 0.0$ ppm) or relative to solvent peaks (^{1}H NMR: $CDCl_3$ $\delta = 7.2$ ppm, $[D_6]$DMSO $\delta = 2.5$ ppm, HOD $\delta = 3.3$ ppm; ^{13}C NMR: $CDCl_3$ $\delta = 77.0$ ppm, $[D_6]$DMSO $\delta = 39.5$ ppm). Multiplicities are denoted as follows: s = singlet, d = doublet, t = triplet, q = quartet, dd = doublet of doublets, ddd = doublet of doublet of doublets, td = triplet of doublets, qd = quartet of doublets, m = multiplet, br = broad and apt = apparently. Coupling constants (*J*) are reported in Hertz (Hz). Mass spectrometric analyses were recorded on Finnigan MAT LCQ MS/MS ESI, AB Sciex TripleTOF 5600 and AB MDS Sciex 4800 MALDI-TOF-TOF mass spectrometers.

HPLC analysis

All HPLC analyses were carried out at 25 °C by using a Prominence Shimadzu System equipped with an LC-20AD solvent delivery unit, SPD-M20A photodiode array detector, SIL-20A$_{HT}$ auto-sampler and CTO-20A column oven. For instrument control and data processing, LabSolutions data managing software (version 5.54 SP2) was utilised. Chiralpak AD (0.46 mm×250 mm) and Chiralcel OJ (0.46 mm×250 mm) columns were obtained from Daicel Chiral Technologies. HPLC-grade *n*-hexane and 2-propanol were obtained from Scharlau Chemie SA. Chiral HPLC separation conditions were determined by obtaining a separation of a standard racemic sample and by applying previously reported parameters if any.

X-ray crystallography of the dirhodium(II) complexes

X-ray-quality crystals of the dirhodium(II) complexes were obtained by dissolving the pure complex in the appropriate solvent (for **5**, green prisms from ethyl acetate/*n*-hexane (1:1); for **6**, green prisms from THF that were violet at the data collection temperature of 100 K; for **7**, green needles from MeOH; for **8**, violet prisms from ACN). The resulting solutions were subjected to sonication and Pasteur pipette filtration followed by slow evaporation of the solvent to yield crystals of the complexes (for $[Rh_2(S\text{-PTAD})_4]$, green prisms were obtained by using the "vapour-diffusion crystallisation" method of *n*-hexane into an EtOAc solution that had been subjected to sonication and Pasteur pipette filtration). Data were collected at −173 °C on crystals mounted on a Hampton Scientific cryoloop at the MX1 (**5**, **8** and $[Rh_2(S\text{-PTAD})_4]$) or MX2 (**6** and **7**) beamlines (Australian Synchrotron, Victoria).[27] The structures were solved by direct methods with SHELXS-97, refined by using full-matrix least-squares methods against F^2 with SHELXL-97[28] and visualised by using X-SEED.[29] Unless described in specific detail below, all non-hydrogen atoms were anisotropically refined, whereas all hydrogen atoms were positioned in calculated locations and refined by using a riding model with fixed C–H distances of 0.95 (sp^2CH), 1.00 (sp^3CH), 0.99 (CH_2) and 0.98 Å (CH_3). The thermal parameters of all hydrogen atoms were estimated as $U_{iso}(H) = 1.2U_{eq}(C)$ except for C*H*$_3$, for which $U_{iso}(H) = 1.5U_{eq}(C)$.

In addition to the general X-ray crystallographic conditions described earlier for data collection and refinement, for **5** and **6** diffuse lattice solvent areas (ethyl acetate for **5** and THF for **6**) were treated with SQUEEZE.[30] For **5**, the rhodium-bound ethyl acetate solvent was apparent in difference maps, which was extensively disordered around the rotational axis. The isotropic refinement model for these solvent molecules required a number of positional and thermal parameter restraints. For **6**, refinement in $P2_12_12$ is presented. A similarly disordered refinement was established in tetragonal *P*4, but this is inconsistent with the systematic absences. Refinement in $P42_12$, which has the same systematic absences as $P2_12_12$, resulted in disordered rhodium centres along the C_2 axis and was not pursued. The rhodium-bound THF molecules were also badly disordered over four sites. Each rhodium axial coordination site featured a similar disorder that was modelled through the use of carbon atoms with 50 and 25% occupancies and EXYZ, EADP and FREE cards to handle the location of hydrogen atoms. All the carbon atoms of the THF molecules were modelled isotropically.

Crystals of **12** suitable for single-crystal X-ray crystallography were obtained by dissolving the compound prepared from $[Rh_2(S\text{-}^{tert}\text{PTTL})_4]$ (**6**) in ethyl acetate/*n*-hexane (1:3). The resulting solution

was subjected to sonication and Pasteur pipette filtration. Colourless crystals were obtained by the slow evaporation of the solvent and were used directly for measurement. Single-crystal X-ray diffraction data were collected at 200 K on a Nonius–KappaCCD diffractometer equipped with graphite-monochromatised $Mo_{K\alpha}$ radiation ($\lambda = 0.71073$ Å).

Crystals of **16** suitable for single-crystal X-ray crystallography were obtained by dissolving the compound prepared from [Rh_2(*S*-^{tert}PTTL)$_4$] (**6**) in IPA. Colourless crystals were obtained by the slow evaporation of the solvent which was used directly for measurement. Single-crystal X-ray diffraction data were collected at 150 K on an Agilent SuperNova Dual diffractometer equipped with mirror-monochromatised $Cu_{K\alpha}$ radiation ($\lambda = 1.54180$ Å).

Crystal data for 5: $C_{104}H_{96}N_4O_{20}Rh_2$, $M = 1927.66$, tetragonal, $a = 21.4840(18)$, $c = 11.661(5)$ Å, $V = 5382(2)$ Å^3, $T = 100$ K, space group $I\bar{4}$ (no. 79), $Z = 2$, 40745 reflections measured, 6413 unique ($R_{int} = 0.0247$), $6289 > 4\sigma(F)$, $R = 0.0416$ (observed), $R_w = 0.1143$ (all data).

Crystal data for 6: $C_{72}H_{92}N_4O_{16}Rh_2{\cdot}2(C_4H_8O)$, $M = 1619.52$, orthorhombic, $a = 19.0510(12)$, $b = 19.0440(10)$, $c = 11.599(3)$ Å, $V = 4208.2(12)$ Å^3, $T = 100$ K, space group $P2_12_12$ (no. 18), $Z = 2$, 93973 reflections measured, 15027 unique ($R_{int} = 0.0528$), $13223 > 4\sigma(F)$, $R = 0.0421$ (observed), $R_w = 0.1160$ (all data).

Crystal data for 7: $C_{66}H_{94}N_4O_{18}Rh_2{\cdot}2(CH_4O)$, $M = 1501.35$, orthorhombic, $a = 8.8180(18)$, $b = 13.414(3)$, $c = 57.659(12)$ Å, $V = 6820(2)$ Å^3, $T = 100$ K, space group $P2_12_12_1$ (no. 19), $Z = 4$, 52260 reflections measured, 15296 unique ($R_{int} = 0.0981$), $11459 > 4\sigma(F)$, $R = 0.0880$ (observed), $R_w = 0.2100$ (all data).

Crystal data for 8: $C_{64}H_{86}N_6O_{16}Rh_2$, $M = 1401.20$, monoclinic, $a = 12.765(5)$, $b = 21.453(4)$, $c = 12.932(3)$ Å, $\beta = 112.262(12)^\circ$, $V = 3277.4(16)$ Å^3, $T = 100$ K, space group $P2_1$ (no. 4), $Z = 2$, 53135 reflections measured, 19812 unique ($R_{int} = 0.0509$), $17763 > 4\sigma(F)$, $R = 0.0348$ (observed), $R_w = 0.0798$ (all data).

Crystal data for [Rh_2(*S*-PTAD)$_4$]: $2(C_{88}H_{96}N_4O_{20}Rh_2){\cdot}C_6H_{14}{\cdot}C_4H_8O_2$, $M = 3645.28$, monoclinic, $a = 19.5350(14)$, $b = 14.2510(15)$, $c = 30.592(2)$ Å, $\beta = 90.6030(10)^\circ$, $V = 8516.1(12)$ Å^3, $T = 100$ K, space group $P2_1$ (no. 4), $Z = 2$, 128848 reflections measured, 39729 unique ($R_{int} = 0.0324$), $38005 > 4\sigma(F)$, $R = 0.0389$ (observed), $R_w = 0.1017$ (all data).

Crystal data for 12: $C_{18}H_{21}O_3P$, $M = 316.34$, orthorhombic, $a = 6.6766(1)$, $b = 15.6794(3)$, $c = 16.3174(3)$ Å, $V = 1708.19(5)$ Å^3, $T = 200$ K, space group $P2_12_12_1$ (no. 19), $Z = 4$, 30661 reflections measured, 3918 unique ($R_{int} = 0.034$), $3605 > 4\sigma(F)$, $R = 0.0345$ (observed), $R_w = 0.0918$ (all data).

Crystal data for 16: $C_{16}H_{13}F_3$, $M = 262.27$, monoclinic, $a = 9.2411(3)$, $b = 5.7885(2)$, $c = 12.0746(5)$ Å, $\beta = 94.319(3)^\circ$, $V = 644.06(4)$ Å^3, $T = 150$ K, space group $P2_1$ (no. 4), $Z = 2$, 11761 reflections measured, 2530 unique ($R_{int} = 0.066$), $2502 > 4\sigma(F)$, $R = 0.0814$ (observed), $R_w = 0.2014$ (all data).

CCDC 1063700 (**5**), 1063701 (**6**), 1433479 (**7**), 1433480 (**8**), 1433481 ([Rh_2(*S*-PTAD)$_4$]), 1433482 (**12**), and 1433483 (**16**) contain the supplementary crystallographic data for this paper. These data are provided free of charge by The Cambridge Crystallographic Data Centre.

Synthetic procedures

Preparation of racemic cyclopropane derivatives: All racemic cyclopropane standards for chiral HPLC analysis were synthesised following the same synthetic procedures designated below with [$Rh_2(OAc)_4$] employed as catalyst. Analytical samples were obtained by purification by preparative TLC.

Synthesis of the new dirhodium(II) carboxylate complexes[25]

General procedure for the preparation of ligands: Triethylamine (TEA; 0.1 equiv) was added to a mixture of the acid anhydride (1.1 equiv) and the L-amino acid (1 equiv) in anhydrous toluene, and the mixture was heated at reflux for 12 h under nitrogen. After that time, the reaction mixture was diluted with ethyl acetate, washed twice with 0.1 M hydrochloric acid solution, dried over anhydrous Na_2SO_4, filtered and concentrated in vacuo. The residue was then purified by silica gel column chromatography using ethyl acetate/*n*-hexane as eluent to afford the corresponding desired product. The amounts of acid anhydride and L-amino acid used are given below.

(*S*)-N-(1-Phenylnaphthalene-2,3-dicarboximido)-*tert*-leucine (*S*-1-Ph-BPTTL, 1): 1-Phenylnaphthalene-2,3-dicarboxylic anhydride (0.47 g, 1.7 mmol), L-*tert*-leucine (0.2 g, 1.6 mmol); colourless oil (0.6 g, 99%). $[\alpha]_D^{25} = -0.35$ ($c = 1$ in $CHCl_3$); $R_f = 0.59$ (ethyl acetate/*n*-hexane, 1:1); ^{1}H NMR (400 MHz, $CDCl_3$): $\delta = 8.30$ (s, 1H; Ar-*H*), 7.98 (d, $J = 7.8$ Hz, 1H; Ar-*H*), 7.70 (d, $J = 8.2$ Hz, 1H; Ar-*H*), 7.62–7.37 (m, 5H; Ar-*H*), 7.30 (m, 2H; Ar-*H*), 4.65 (s, 1H; *CH*N), 1.08 ppm (s, 9H; C(CH_3)$_3$); ^{13}C NMR (100 MHz, $CDCl_3$): $\delta = 172.9$ (*C*OOH), 167.6, 166.9 (2×*C*ON), 140.6, 135.5, 134.2, 130.3, 129.9, 129.2, 129.0, 128.6, 128.5, 128.2, 128.1, 127.2, 124.7, 123.1 (16×Ar-*C*), 60.0 (NCH), 35.1 (*C*(CH_3)$_3$), 28.1 ppm (C(*C*H_3)$_3$); IR (film): $\tilde{\nu} = 2962$, 1709, 1368, 1241, 1114, 767, 699 cm^{-1}; MS (ESI): *m/z*: calcd for $[C_{24}H_{21}NO_4+H]^+$: 388.15; found: 388.16; calcd for $[C_{24}H_{20}NO_4-CO_2]^-$: 342.15; found: 342.15.

(*S*)-N-(4-*tert*-Butylphthalimido)-*tert*-leucine (*S*-^{tert}PTTL, 2): 4-*tert*-Butylphthalic anhydride (0.514 g, 2.52 mmol), L-*tert*-leucine (0.3 g, 2.29 mmol); colourless oil (0.7 g, 96%); $[\alpha]_D^{25} = -0.35$ ($c = 1$ in $CHCl_3$); $R_f = 0.7$ (ethyl acetate/*n*-hexane, 1:1); ^{1}H NMR (400 MHz, $CDCl_3$): $\delta = 7.88$–7.71 (m, 3H; Ar-*H*), 4.69 (s, 1H; NC*H*), 1.34 (s, 9H; C(CH_3)$_3$), 1.15 ppm (s, 9H; C(CH_3)$_3$); ^{13}C NMR (100 MHz, $CDCl_3$): $\delta = 173.3$ (*C*OOH), 168.4, 168.0 (2×*C*ON), 158.9, 131.8, 131.3, 128.9, 123.4, 120.8 (6×Ar-*C*), 59.8 (NCH), 35.7, 35.6 (2×*C*(CH_3)$_3$), 31.1, 27.9 ppm (2×C(*C*H_3)$_3$); IR (film): $\tilde{\nu} = 2963$, 1711, 1372, 1101, 908, 729 cm^{-1}; MS (ESI): *m/z*: calcd for $[C_{18}H_{23}NO_4+H]^+$ 318.17; found: 318.17; calcd for $[C_{18}H_{22}NO_4-CO_2]^-$ 272.17; found: 272.17.

(*S*)-N-(*endo*-Bicyclo[2.2.1]hept-5-ene-2,3-dicarboximido)-*tert*-leucine (*S*-BHTL, 3): *endo-cis*-5-Norbornene-2,3-dicarboxylic anhydride (0.413 g, 2.52 mmol), L-*tert*-leucine (0.3 g, 2.29 mmol); white solid (0.57 g, 90%); $[\alpha]_D^{25} = -0.55$ ($c = 1$ in $CHCl_3$); $R_f = 0.30$ (ethyl acetate/*n*-hexane, 1:1); ^{1}H NMR (400 MHz, $CDCl_3$): $\delta = 6.13$–6.09 (ddd, 2H; C*H*=C*H*), 4.34 (s, 1H; C*H*N), 3.40 (br s, 2H; 2×C*H*), 3.35–3.30 (m, 2H; 2×C*H*), 1.63 (dd, $J = 74.8$, 8.8 Hz, 2H; CH_2), 1.02 ppm (s, 9H; C(CH_3)$_3$); ^{13}C NMR (100 MHz, $CDCl_3$): $\delta = 177.4$, 177.3 (2×*C*ON), 172.4 (*C*OOH), 135.2 (=*C*H), 134.5 (=*C*H), 60.2 (NCH), 52.5 (*C*H_2), 46.0, 45.7 (2×*C*H), 45.3, 44.9 (2×*C*H), 35.4 (*C*(CH_3)$_3$), 27.8 ppm (C(*C*H_3)$_3$); IR (film): $\tilde{\nu} = 3294$, 2960, 2870, 1739, 1687, 1380, 1339, 1169, 1145, 713 cm^{-1}; MS (ESI): *m/z*: calcd for $[C_{15}H_{19}NO_4+H]^+$; 278.13; found: 278.13. Recrystallised from hot MeOH.

(*S*)-N-(*endo*-Bicyclo[2.2.2]oct-5-ene-2,3-dicarboximido)-*tert*-leucine (*S*-BOTL, 4): *endo*-Bicyclo[2.2.2]oct-5-ene-2,3-dicarboxylic anhydride (0.5 g, 2.8 mmol), L-*tert*-leucine (0.3 g, 2.3 mmol); white solid (0.65 g, 98%); $[\alpha]_D^{25} = -0.45$ ($c = 1$ in $CHCl_3$); $R_f = 0.31$ (ethyl acetate/*n*-hexane, 1:1); ^{1}H NMR (400 MHz, $CDCl_3$): $\delta = 6.19$ (m, 2H; C*H*=C*H*), 4.43 (s, 1H; C*H*N), 3.17 (s, 2H; 2×C*H*), 2.90 (qd, $J = 8.4$, 2.9 Hz, 2H; 2×C*H*), 1.61 (d, $J = 7.7$ Hz, 2H; CH_2), 1.39 (d, $J = 8.8$ Hz, 2H; CH_2), 1.05 ppm (s, 9H; C(CH_3)$_3$); ^{13}C NMR (100 MHz, $CDCl_3$): $\delta = 178.8$, 178.6 (2×*C*ON), 172.3 (*C*OOH), 132.8 (=*C*H), 132.4 (=*C*H), 60.2 (NCH), 44.3, 43.9 (2×*C*H), 35.6 (*C*(CH_3)$_3$), 31.8, 31.5 (2×*C*H), 27.8 (C(CH_3)$_3$), 23.7, 23.6 ppm (2×*C*H_2); IR (film): $\tilde{\nu} = 3294$, 2958, 2870, 1746, 1683, 1389, 1366, 1166, 1145, 701 cm^{-1}; MS (ESI): *m/z*: calcd for $[C_{16}H_{21}NO_4+H]^+$ 292.15; found: 292.15; calcd for

$[C_{16}H_{20}NO_4-CO_2]^-$ 246.15; found: 246.15. Recrystallised from hot MeOH.

General procedure for ligand exchange: A mixture of the carboxylic acid ligand (6 equiv) and dirhodium(II) tetraacetate ($[Rh_2(OAc)_4]$, 1 equiv) in dry chlorobenzene was heated at reflux for 24 h under nitrogen using a Soxhlet extractor fitted with a thimble containing a dry mixture of Na_2CO_3 and sand (1:1) for trapping the eliminated acetic acid molecules. After that time, the solvent was evaporated in vacuo and the residue was redissolved in DCM, washed with a saturated solution of $NaHCO_3$, dried over anhydrous Na_2SO_4, filtered and concentrated in vacuo. The green residue was then purified by silica gel column chromatography using ethyl acetate/*n*-hexane as eluent. The pure products were dried overnight under vacuum at 50 °C before analysis. The amounts of carboxylic acid ligand and $[Rh_2(OAc)_4]$ are given below.

Dirhodium(II,II) tetrakis[(*S*)-N-(1-phenylnaphthalene-2,3-dicarboximido)-*tert*-leucinate] ($[Rh_2(S\text{-1-Ph-BPTTL})_4]$, 5): Ligand (0.621 g, 1.60 mmol), $[Rh_2(OAc)_4]$ (0.12 g, 0.27 mmol); green solid (0.31 g, 67%); $R_f = 0.77$ (ethyl acetate/*n*-hexane, 1:1); ^{1}H NMR (400 MHz, $CDCl_3$): $\delta = 8.07$ (s, 4H; Ar-*H*), 7.60 (d, $J = 8.2$ Hz, 8H; Ar-*H*), 7.51–7.30 (m, 24H; Ar-*H*), 7.12 (d, $J = 6.9$ Hz, 4H; Ar-*H*), 4.92 (s, 4H; 4×C*H*N), 1.19–1.16 ppm (m, 36H; 4×C(CH_3)$_3$); ^{13}C NMR (100 MHz, $CDCl_3$): $\delta = 186.2$ (*C*OO), 166.3, 165.5 (*C*ON), 138.2, 134.5, 134.1, 133.8, 129.6, 129.2, 128.9, 127.4, 127.2, 127.0, 126.8, 126.6, 123.4, 122.9 (Ar-*C*), 60.4 (NCH), 34.7 (*C*(CH_3)$_3$), 27.0 ppm (C(*C*H$_3$)$_3$); IR (film): $\tilde{\nu} = 2962$, 1709, 1617, 1397, 1365, 1340, 1260, 1109, 1030, 801, 761, 696 cm^{-1}; MS (ESI): *m/z*: calcd for $[C_{96}H_{80}N_4O_{16}Rh_2+7H]^+$: 1758.4; found: 1758.1; calcd for $[C_{96}H_{80}N_4O_{16}Rh_2+5H-C_{24}H_{20}NO_4]^+$: 1369.2; found: 1369.1; calcd for $[C_{96}H_{80}N_4O_{16}Rh_2+2H-2C_{24}H_{20}NO_4]^+$: 980.1; found: 980.1; calcd for $[C_{96}H_{80}N_4O_{16}Rh_2-3C_{24}H_{20}NO_4-H]^+$: 608.9; found: 608.9; calcd for $[C_{24}H_{20}NO_4-CO_2]^-$: 342.1) found: 341.7.

Dirhodium(II) tetrakis[(*S*)-N-(4-*tert*-butylphthalimido)-*tert*-leucinate] ($[Rh_2(S\text{-}^{tert}PTTL)_4]$, 6): Ligand (0.645 g, 2.032 mmol), $[Rh_2(OAc)_4]$ (0.150 g, 0.339 mmol); green solid (0.35 g, 71%); $R_f = 0.50$ (ethyl acetate/*n*-hexane, 1:2); ^{1}H NMR (400 MHz, $CDCl_3$): $\delta = 7.85$ (brs, 4H; Ar-*H*), 7.67–7.62 (m, 8H; Ar-*H*), 4.88 (s, 4H; 4 NC*H*), 1.35 (s, 36H; 4 C(CH_3)$_3$), 1.11 ppm (s, 36H; 4 C(CH_3)$_3$); ^{13}C NMR (100 MHz, $CDCl_3$): $\delta = 187.1$ (*C*OO), 172.1, 168.2 (*C*ON), 158.0, 132.1, 130.5, 129.4, 122.9, 120.5 (Ar-*C*), 61.26 (NCH), 35.6, 35.5 (2 *C*(CH_3)$_3$), 31.1, 27.9 ppm (2 C(*C*H$_3$)$_3$); IR (film): $\tilde{\nu} = 2959$, 1713, 1612, 1366, 1103, 752, 693 cm^{-1}; MS (ESI): *m/z*: calcd for $[C_{72}H_{88}N_4O_{16}Rh_2+6H]^+$: 1476.4; found: 1476.8; calcd for $[C_{72}H_{88}N_4O_{16}Rh_2+4H-C_{18}H_{22}NO_4]^+$: 1158.3; found: 1158.1; calcd for $[C_{72}H_{88}N_4O_{16}Rh_2+2H-2\times C_{18}H_{22}NO_4]^+$: 840.1; found: 839.5.

Dirhodium(II,II) tetrakis[(*S*)-N-(*endo*-bicyclo[2.2.2]oct-5-ene-2,3-dicarboximido)-*tert*-leucinate] ($[Rh_2(S\text{-BOTL})_4]$, 7): Ligand (0.53 g, 1.82 mmol), $[Rh_2(OAc)_4]$ (0.13 g, 0.30 mmol); green solid (0.38 g, 92%); $R_f = 0.34$ (ethyl acetate/*n*-hexane, 1:1); ^{1}H NMR (400 MHz, $CDCl_3$): $\delta = 6.15$ (brs, 8H; C*H*=C*H*), 4.41 (brs, 4H; 4 C*H*N), 3.11 (brs, 8H; 8 C*H*), 2.73 (brs, 8H; 8 C*H*), 1.56 (brs, 8H; 4 CH_2), 1.36 (brs, 8H; 4 CH_2), 1.05 ppm (s, 36H; 4 C(CH_3)$_3$); ^{13}C NMR (100 MHz, $CDCl_3$): $\delta = 185.5$, 185.3 (*C*OO), 177.8, 176.2 (*C*ON), 132.9, 132.0, 131.8, 129.6, 128.7, 127.6, 127.0, 125.3 (CH=*C*H), 60.7 (NCH), 43.77, 43.15, 42.9, 42.7, 42.5 (*C*H), 34.4 (*C*(CH_3)$_3$), 30.6 (*C*H), 26.8 (C(*C*H$_3$)$_3$), 22.8 ppm (*C*H$_2$); IR (film): $\tilde{\nu} = 2953$, 2868, 1703, 1612, 1375, 1174, 781, 695 cm^{-1}; MS (ESI): *m/z*: calcd for $[C_{64}H_{86}N_4O_{16}Rh_2+6H]^+$: 1372.4; found: 1372.3; calcd for $[C_{64}H_{86}N_4O_{16}Rh_2+4H-C_{16}H_{20}NO_4]^+$: 1080.2; found: 1079.7; calcd for $[C_{64}H_{86}N_4O_{16}Rh_2+H-2C_{16}H_{20}NO_4]^+$: 787.1; found: 787.2.

Dirhodium(II,II) tetrakis[(*S*)-N-(*endo*-bicyclo[2.2.1]hept-5-ene-2,3-dicarboximido)-*tert*-leucinate] ($[Rh_2(S\text{-BHTL})_4]$, 8): Ligand (0.49 g, 1.77 mmol), $[Rh_2(OAc)_4]$ (0.13 g, 0.29 mmol); green solid (0.32 g, 83%); $R_f = 0.22$ (ethyl acetate/*n*-hexane, 1:1); ^{1}H NMR (400 MHz, $CDCl_3$): $\delta = 6.32$–5.86 (m, 8H; 4 C*H*=C*H*), 4.70–3.96 (m, 4H; 4 C*H*N), 3.38–3.10 (m, 16H; 16 C*H*), 1.79–1.41 (m, 8H; 4 CH_2), 0.87 ppm (brs, 36H; 4 C(CH_3)$_3$); ^{13}C NMR (100 MHz, $CDCl_3$): $\delta = 186.0$ (*C*OO), 176.4, 175.2 (*C*ON), 135.1, 132.0 (*C*H=*C*H), 60.9 (NCH), 50.7 (*C*H$_2$), 45.5, 44.4 (*C*H), 43.9 43.7 (*C*H), 34.2 (*C*(CH_3)$_3$), 26.8 ppm (C(*C*H$_3$)$_3$); IR (film): $\tilde{\nu} = 2961$, 1703, 1610, 1398, 1372, 1345, 1172, 1039, 803, 778, 692 cm^{-1}; MS (ESI): *m/z*: calcd for $[C_{60}H_{80}N_4O_{16}Rh_2+6H]^+$: 1316.3; found: 1315.9; calcd for $[C_{60}H_{80}N_4O_{16}Rh_2+5H-C_5H_6]^+$: 1249.3; found: 1249.6; calcd for $[C_{60}H_{80}N_4O_{16}Rh_2+5H-2C_5H_6]^+$: 1183.2; found: 1183.2; calcd for $[C_{60}H_{80}N_4O_{16}Rh_2+4H-C_{15}H_{20}NO_4]^+$: 1038.2; found: 1037.5; calcd for $[C_{60}H_{80}N_4O_{16}Rh_2+3H-C_{15}H_{20}NO_4-C_5H_6]^+$: 971.1; found: 971.1; calcd for $[C_{60}H_{80}N_4O_{16}Rh_2+H-2C_{15}H_{20}NO_4]^+$: 759.0; found: 759.1.

General procedure for the preparation of cyclopropylphosphonate derivatives: A solution of α-diazobenzylphosphonate (1 equiv) in 2,2-DMB (10 mL) was added dropwise through a syringe pump to a stirred solution of alkene (5 equiv) and dirhodium(II) catalyst (0.01 equiv) in 2,2-DMB (3 mL) heated at reflux (59 °C) under nitrogen for 10 min. After the addition, the reaction was further heated at reflux until TLC indicated complete consumption of the diazo starting material. The diastereomeric ratio (d.r.) of the generated product was determined by ^{1}H NMR analysis of the crude mixture. The product was purified by preparative TLC (ethyl acetate/*n*-hexane) and the enantiomeric excess (*ee*%) of the product was determined by chiral HPLC analysis.

General procedure for the preparation of cyclopropylphosphonate derivatives using $[Rh_2(S\text{-}^{tert}PTTL)_4]$ (6): A solution of α-diazobenzylphosphonate (1 equiv) in 2,2-DMB (10 mL) was added dropwise through a syringe pump to a stirred solution of alkene (5 equiv) and $[Rh_2(S\text{-}^{tert}PTTL)_4]$ (**6**; 0.01 equiv) in 2,2-DMB (3 mL) under nitrogen over a period of 10 min. After the addition, the reaction was stirred at room temperature until TLC indicated a complete consumption of the diazo starting material. The diastereomeric ratio (d.r.) of the generated product was determined by ^{1}H NMR analysis of the crude mixture. The product was purified by preparative TLC (ethyl acetate/*n*-hexane) and the enantiomeric excess (*ee*%) of the product was determined by chiral HPLC analysis.

Dimethyl (*E*)-1,2-diphenylcyclopropylphosphonate (9):[31] Colourless oil; $[\alpha]_D^{25} = -0.25$ ($c = 0.53$ in $CHCl_3$, 98% *ee*); $R_f = 0.15$ (ethyl acetate/*n*-hexane, 1:1); ^{1}H NMR (400 MHz, $CDCl_3$): $\delta = 7.00$ (m, 3H; Ar-*H*), 6.99 (m, 5H; Ar-*H*), 6.68 (m, 2H; Ar-*H*), 3.67 (d, $J_{HP} = 10.5$ Hz, 3H; OC*H*$_3$), 3.62 (d, $J_{HP} = 10.5$ Hz, 3H; OC*H*$_3$), 2.95 (ddd, $J_{HP} = 16.5$, $J = 8.8$, 6.7 Hz, 1H; C*H*), 1.99 (ddd, $J_{HP} = 17.3$, $J = 8.8$, 5.1 Hz, 1H; C*H*$_2$), 1.66 ppm (ddd, $J_{HP} = 12.2$, $J = 6.7$, 5.1 Hz, 1H; C*H*$_2$). The spectroscopic data are consistent with previously reported data.[31] The enantiomeric excess was determined by chiral HPLC (Chiralcel OJ column, 25×0.46 cm, 2% 2-propanol in *n*-hexane (v/v%); 1 mL min^{-1}, 220 nm, $t_1 = 18$ min, $t_2 = 21$ min).

Dimethyl (*E*)-1-phenyl-2-(*p*-chlorophenyl)cyclopropylphosphonate (10):[31b] Colourless oil; $[\alpha]_D^{25} = -0.54$ ($c = 0.87$ in $CHCl_3$, 98% *ee*); $R_f = 0.11$ (ethyl acetate/*n*-hexane, 1:1); ^{1}H NMR (400 MHz, $CDCl_3$): $\delta = 7.14$–7.11 (m, 3H; Ar-*H*), 7.04 (m, 2H; Ar-*H*), 7.01 (d, $J = 8.5$ Hz, 2H; Ar-*H*), 6.64 (d, $J = 8.4$ Hz, 2H; Ar-*H*), 3.70 (d, $J_{HP} = 10.6$ Hz, 3H; OC*H*$_3$), 3.66 (d, $J_{HP} = 10.6$ Hz, 3H; OC*H*$_3$), 2.96 (ddd, $J_{HP} = 16.5$, $J = 8.8$, 6.7 Hz, 1H; C*H*), 2.06 (ddd, $J_{HP} = 17.4$, $J = 9.0$, 5.3 Hz, 1H; C*H*$_2$), 1.66 (ddd, $J_{HP} = 12.4$, $J = 6.5$, 5.3 Hz, 1H; C*H*$_2$). The spectroscopic data are consistent with previously reported data.[31b] The enantiomeric excess was determined by chiral HPLC (Chiralcel OJ column, 25×0.46 cm, 8% 2-propanol in *n*-hexane (v/v%); 1 mL min^{-1}, 220 nm, $t_1 = 10$ min, $t_2 = 12$ min).

Dimethyl (*E*)-1-phenyl-2-(*p*-methoxyphenyl)cyclopropylphosphonate (11):[31b] Colourless oil; $[\alpha]_D^{25} = -0.57$ ($c = 1$ in $CHCl_3$, 99% *ee*); $R_f = 0.11$ (ethyl acetate/*n*-hexane, 1:1); ^{1}H NMR (400 MHz, $CDCl_3$): $\delta = 7.12–7.10$ (m, 3H; Ar-*H*), 7.05 (m, 2H; Ar-*H*), 6.62 (dd, $J = 23.0$, 8.9 Hz, 4H; Ar-*H*), 3.71 (d, $J_{HP} = 10.6$ Hz, 3H; OCH_3), 3.68 (s, 3H; OCH_3), 3.66 (d, $J_{HP} = 10.6$ Hz, 3H; OCH_3), 2.96 (ddd, $J_{HP} = 16.1$, $J = 9.1$, 6.6 Hz, 1H; C*H*), 2.03 (ddd, $J_{HP} = 17.5$, $J = 9.1$, 5.2 Hz, 1H; CH_2), 1.64 ppm (ddd, $J_{HP} = 12.4$, $J = 6.5$, 5.3 Hz, 1H; CH_2). The spectroscopic data are consistent with previously reported data.[31b] The enantiomeric excess was determined by chiral HPLC (Chiralcel OJ column, 25×0.46 cm, 3% 2-propanol in *n*-hexane (v/v%); 1 mL min^{-1}, 220 nm, $t_1 = 37$ min, $t_2 = 42$ min).

Dimethyl (*E*)-1-phenyl-2-(*p*-methylphenyl)cyclopropylphosphonate (12): White solid; $[\alpha]_D^{25} = -0.57$ ($c = 0.93$ in $CHCl_3$, 99% *ee*); $R_f = 0.17$ (ethyl acetate/*n*-hexane, 1:1); ^{1}H NMR (400 MHz, $CDCl_3$): $\delta = 7.13–7.10$ (m, 3H; Ar-*H*), 7.07–7.04 (m, 2H; Ar-*H*), 6.85 (d, $J = 7.8$ Hz, 2H; Ar-*H*), 6.61 (d, $J = 8.2$ Hz, 2H; Ar-*H*), 3.72 (d, $J_{HP} = 10.6$ Hz, 3H; OCH_3), 3.66 (d, $J_{HP} = 10.6$ Hz, 3H; OCH_3), 2.97 (ddd, $J_{HP} = 16.1$, $J = 9.1$, 6.6 Hz, 1H; C*H*), 2.19 (s, 3H; CH_3), 2.03 (ddd, $J_{HP} = 17.5$, $J = 9.0$, 5.1 Hz, 1H; CH_2), 1.67 ppm (ddd, $J_{HP} = 12.5$, $J = 6.6$, 5.1 Hz, 1H; CH_2). The enantiomeric excess was determined by chiral HPLC (Chiralcel OJ column, 25×0.46 cm, 3% 2-propanol in *n*-hexane (v/v%); 1 mL min^{-1}, 220 nm, $t_1 = 12$ min, $t_2 = 15$ min).

Dimethyl (*E*)-1-phenyl-2-(1-naphthyl)cyclopropylphosphonate (13): Colourless oil; $[\alpha]_D^{25} = -0.24$ ($c = 0.5$ in $CHCl_3$, 98% *ee*); $R_f = 0.14$ (ethyl acetate/*n*-hexane, 1:1); ^{1}H NMR (400 MHz, $CDCl_3$): $\delta = 7.72–7.53$ (m, 2H; Ar-*H*), 7.50 (d, $J = 7.50$ Hz, 1H; Ar-*H*), 7.35 (m, 2H; Ar-*H*), 7.29 (s, 1H; Ar-*H*), 7.07 (m, 4H; Ar-*H*), 6.76 (dd, $J = 8.5$, 1.8 Hz, 1H; Ar-*H*), 3.75 (d, $J_{HP} = 10.6$ Hz, 3H; OCH_3), 3.70 (d, $J_{HP} = 10.6$ Hz, 3H; OCH_3), 3.16 (ddd, $J_{HP} = 16.1$, $J = 9.1$, 6.6 Hz, 1H; C*H*), 2.14 (ddd, $J_{HP} = 17.5$, $J = 9.0$, 5.3 Hz, 1H; CH_2), 1.85 ppm (ddd, $J_{HP} = 12.5$, $J = 6.6$, 5.1 Hz, 1H; CH_2). The enantiomeric excess was determined by chiral HPLC (Chiralpak AD column, 25×0.46 cm, 1% 2-propanol in *n*-hexane (v/v%); 2 mL min^{-1}, 220 nm, $t_1 = 36$ min, $t_2 = 42$ min).

Diethyl (*E*)-1,2-diphenylcyclopropylphosphonate (14):[31b] Colourless oil; $[\alpha]_D^{25} = -0.11$ ($c = 0.4$ in $CHCl_3$, 92% *ee*); $R_f = 0.26$ (ethyl acetate/*n*-hexane, 1:1); ^{1}H NMR (400 MHz, $CDCl_3$): $\delta = 7.11–7.07$ (m, 4H; Ar-*H*), 7.06–7.01 (m, 4H; Ar-*H*), 6.72 (m, 2H; Ar-*H*), 4.11–3.95 (m, 4H; 2 OCH_2CH_3), 2.98 (ddd, $J_{HP} = 16.5$, $J = 8.8$, 6.5 Hz, 1H; C*H*), 1.99 (ddd, $J_{HP} = 17.5$, $J = 9.0$, 5.1 Hz, 1H; CH_2), 1.68 (ddd, $J_{HP} = 12.2$, $J = 6.7$, 5.1 Hz, 1H; CH_2), 1.26 (td, $J = 7.0$, 0.4 Hz, 3H; OCH_2CH_3), 1.22 ppm (td, $J = 7.0$, 0.5 Hz, 3H; OCH_2CH_3). The spectroscopic data are consistent with previously reported data.[31b] The enantiomeric excess was determined by chiral HPLC (Chiralpak AD column, 25×0.46 cm, 0.6% 2-propanol in *n*-hexane (v/v%); 0.8 mL min^{-1}, 220 nm, $t_1 = 69$ min, $t_2 = 76$ min).

Diisopropyl (*E*)-1,2-diphenylcyclopropylphosphonate (15):[31b] Colourless oil; $R_f = 0.40$ (ethyl acetate/*n*-hexane, 1:1); ^{1}H NMR (400 MHz, $CDCl_3$): $\delta = 7.08$ (m, 5H; Ar-*H*), 7.02 (m, 3H; Ar-*H*), 6.73 (m, 2H; Ar-*H*), 4.67–4.56 (m, 2H; 2 $CH(CH_3)_2$), 2.95 (ddd, $J_{HP} = 16.8$ Hz, $J = 8.9$, 6.5 Hz, 1H; C*H*), 2.02 (ddd, $J_{HP} = 17.5$, $J = 8.9$, 5.1 Hz, 1H; CH_2), 1.67 (ddd, $J_{HP} = 12.4$ Hz, $J = 6.5$, 5.0 Hz, 1H; CH_2), 1.27 (d, $J = 2.0$ Hz, 3H; $CH(CH_3)_2$), 1.25 (d, $J = 2.0$ Hz, 3H; $CH(CH_3)_2$), 1.23 (d, $J = 6.2$ Hz, 3H; $CH(CH_3)_2$), 1.19 ppm (d, $J = 6.2$ Hz, 3H; $CH(CH_3)_2$). The spectroscopic data are consistent with previously reported data.[31b] The enantiomeric excess was determined by chiral HPLC (Chiralpak AD column, 25×0.46 cm, 0.6% 2-propanol in *n*-hexane (v/v%); 0.8 mL min^{-1}, 220 nm, $t_1 = 49$ min, $t_2 = 54$ min).

(*E*)-1-Trifluoromethyl-1,2-diphenylcyclopropane (16):[7] 1-Phenyl-2,2,2-trifluorodiazoethane (1.0 equiv) dissolved in dry and degassed TFT (2 mL) was added dropwise to a solution of the styrene (5.0 equiv) and dirhodium(II) catalyst (0.02 equiv) in dry and degassed TFT (3 mL) under nitrogen over a period of 10 min by using a syringe pump. The reaction was stirred for another hour, after which time the reaction solvent was removed under reduced pressure. The diastereomeric ratio (d.r.) of the generated product was determined by ^{1}H NMR analysis of the crude mixture. The product was purified by preparative TLC using *n*-hexane as eluent. White solid; $R_f = 0.29$ (*n*-hexane); ^{1}H NMR (400 MHz, $CDCl_3$): $\delta = 7.13–6.99$ (m, 8H; Ar-*H*), 6.71–6.69 (m, 2H; Ar-*H*), 2.77 (dd, $J = 9.6$, 7.0 Hz, 1H; C*H*), 1.81 (dd, $J = 9.6$, 5.9 Hz, 1H; CH_2), 1.61 ppm (m, 1H; CH_2). The spectroscopic data are consistent with previously reported data.[7] The enantiomeric excess was determined by chiral HPLC (Chiralcel OJ column, 25×0.46 cm, 1% 2-propanol in *n*-hexane (v/v%); 0.8 mL min^{-1}, 220 nm, $t_1 = 6.5$ min, $t_2 = 7.8$ min).

General procedure for the preparation of cyclopropanecarboxylates: The diazo compound (1.0 equiv) dissolved in the same dry and degassed solvent was added dropwise through a syringe pump to a solution of styrene (5.0 equiv) and dirhodium(II) catalyst (0.01 equiv) in dry and degassed solvent under nitrogen over a period of 10 min. After the addition, the mixture was stirred for at least 1 h. When the diazo compound was fully consumed, as indicated by TLC, the reaction solvent was removed in vacuo. The diastereomeric ratio (d.r.) of the generated product was determined by ^{1}H NMR analysis of the crude mixture. The product was purified by preparative TLC using ethyl acetate/*n*-hexane and the enantiomeric excess (*ee*%) of the product was determined by chiral HPLC analysis.

Methyl (*E*)-1-(*p*-methoxyphenyl)-2-phenylcyclopropanecarboxylate (17):[5] Colourless oil; $R_f = 0.52$ (ethyl acetate/*n*-hexane, 1:4); ^{1}H NMR (400 MHz, $CDCl_3$): $\delta = 7.10–7.07$ (m, 3H; Ar-*H*), 6.95 (d, $J = 8.8$ Hz, 2H; Ar-*H*), 6.80–6.77 (m, 2H; Ar-*H*), 6.68 (d, $J = 8.8$ Hz, 2H; Ar-*H*), 3.74 (s, 3H; CH_3), 3.68 (s, 3H; CH_3), 3.09 (dd, $J = 9.2$, 7.6 Hz, 1H; C*H*), 2.14 (dd, $J = 9.2$, 4.8 Hz, 1H; CH_2), 1.84 ppm (dd, $J = 7.2$, 4.8 Hz, 1H; CH_2). The spectroscopic data are consistent with previously reported data.[5] The enantiomeric excess was determined by chiral HPLC (Chiralcel OD-H column, 25×0.46 cm, 0.7% 2-propanol in *n*-hexane (v/v%); 1 mL min^{-1}, 220 nm, $t_1 = 13$ min, $t_2 = 23$ min).

Methyl (*E*)-1,2-diphenylcyclopropanecarboxylate (18):[5,32] White solid; m.p. 60–62 °C; $R_f = 0.30$ (ethyl acetate/*n*-hexane, 1:10); ^{1}H NMR (400 MHz, $CDCl_3$): $\delta = 7.13–6.75$ (m, 10H; Ar-*H*), 3.66 (s, 3H; CH_3), 3.11 (dd, $J = 9.3$, 7.3 Hz, 1H; C*H*), 2.13 (dd, $J = 9.3$, 4.9 Hz, 1H; CH_2), 1.88 ppm (dd, $J = 7.3$, 4.9 Hz, 1H; CH_2). The spectroscopic data are consistent with previously reported data.[5,32] The enantiomeric excess was determined by chiral HPLC (Chiralcel OJ column, 25×0.46 cm, 0.5% 2-propanol in *n*-hexane (v/v%); 1 mL min^{-1}, 220 nm, $t_1 = 14$ min, $t_2 = 20$ min).

Methyl (*E*)-2-phenyl-1-[(*Z*)-styryl]cyclopropane-1-carboxylate (19):[33] White solid; m.p. 58–61 °C; $R_f = 0.63$ (ethyl acetate/*n*-hexane, 1:3); ^{1}H NMR (400 MHz, $CDCl_3$): $\delta = 7.17–7.04$ (m, 10H; Ar-*H*), 6.26 (d, $J =$ Hz, 1H; C*H*=CH), 6.05 (d, $J =$ Hz, 1H; CH=C*H*), 3.68 (s, 3H; CH_3), 2.93 (dd, $J = 9.0$, 7.5 Hz, 1H; C*H*), 1.94 (dd, $J = 9.2$, 5.0 Hz, 1H; CH_2), 1.75 ppm (dd, $J = 9.2$, 5.0 Hz, 1H; CH_2). The spectroscopic data are consistent with previously reported data.[33] The enantiomeric excess was determined by chiral HPLC (Chiralcel OJ column, 25×0.46 cm, 1.5% 2-propanol in *n*-hexane (v/v%); 1 mL min^{-1}, 254 nm, $t_1 = 15$ min, $t_2 = 21$ min).

(*E*)-1,2-Diphenylcyclopropanecarbonitrile (20):[6,34] α-Diazo-2-phenylacetonitrile (1 equiv) dissolved in dry and degassed toluene (2 mL) was added dropwise through a syringe pump to a stirred solution of styrene (5 equiv) and dirhodium(II) catalyst (0.02 equiv) in dry and degassed toluene (3 mL) maintained at −78 °C and under nitrogen over a period of 10 min . The orange reaction mixture was allowed to slowly warm up to ~20 °C, during which time, the colour of the mixture returned back to green. The solvent was then removed in vacuo and the diastereomeric ratio (d.r.) of the

generated product was determined by ^{1}H NMR analysis of the residue. The product was purified by preparative TLC using diethyl ether/*n*-hexane (1:10) as eluent. White solid; $R_f = 0.32$ (diethyl ether/*n*-hexane, 1:9); ^{1}H NMR (400 MHz, $CDCl_3$): $\delta = 7.17–7.01$ (m, 8H; Ar-*H*), 6.82–6.80 (m, 2H; Ar-*H*), 3.09 (t, $J = 8.6$ Hz, 1H; C*H*), 2.14–2.00 ppm (m, 2H; CH_2). The enantiomeric excess was determined by chiral HPLC (Chiralcel OD column, 25×0.46 cm, 0.8% 2-propanol in *n*-hexane (v/v%); 1 mL min^{-1}, 220 nm, $t_1 = 19$ min, $t_2 = 29$ min).

(*Z*)-1,2-Diphenylcyclopropanecarbonitrile: White solid; $R_f = 0.32$ (diethyl ether/*n*-hexane, 1:9); ^{1}H NMR (400 MHz, $CDCl_3$): $\delta = 7.34–7.23$ (m, 10H; Ar-*H*), 2.72 (t, $J = 8.4$ Hz, 1H; C*H*), 2.06–1.91 ppm (m, 2H; CH_2). The enantiomeric excess was determined by chiral HPLC (Chiralcel OD column, 25×0.46 cm, 0.8% 2-propanol in *n*-hexane (v/v%); 1 mL min^{-1}, 220 nm, $t_1 = 22$ min, $t_2 = 36$ min).

Acknowledgements

The authors gratefully acknowledge the W. J. Weeden Scholarships Program at the University of Canberra, Australia, for the Ph. D. scholarship offered to Dr. Frady Gamal Adly Gouany. The authors acknowledge the role of Dr. Tony Willis from the Australian National University in obtaining the X-ray crystallographic data of some of the prepared cyclopropane products. Data for the structures of the catalysts were obtained on the MX1/MX2 beamlines at the Australian Synchrotron, Victoria, Australia.

Keywords: asymmetric synthesis · carbenoids · chiral catalysis · cyclopropanation · rhodium

[1] a) F. G. Adly, A. Ghanem, *Chirality* **2014**, *26*, 692–711; b) M. El-Deftar, F. G. Adly, M. G. Gardiner, A. Ghanem, *Curr. Org. Chem.* **2012**, *16*, 1808–1836; c) Y. Deng, H. Qiu, H. D. Srinivas, M. P. Doyle, *Curr. Org. Chem.* **2016**, *20*, 61–81; d) A. F. Trindade, J. A. Coelho, C. A. Afonso, L. F. Veiros, P. M. Gois, *ACS Catal.* **2012**, *2*, 370–383; e) P. Srivastava, H. Yang, K. Ellis-Guardiola, J. C. Lewis, *Nat. Commun.* **2015**, *6*, 7789.

[2] a) J. Hansen, H. M. L. Davies, *Coord. Chem. Rev.* **2008**, *252*, 545–555; b) C. A. Merlic, A. L. Zechman, *Synthesis* **2003**, 1137–1156.

[3] a) H. Tsutsui, M. Matsuura, K. Makino, S. Nakamura, M. Nakajima, S. Kkitagaki, S. Hashimoto, *Isr. J. Chem.* **2001**, *41*, 283–295; b) T. Takahashi, H. Tsutsui, M. Tamura, S. Kitagaki, M. Nakajima, S. Hashimoto, *Chem. Commun.* **2001**, 1604–1605; c) K. Minami, H. Saito, H. Tsutsui, H. Nambu, M. Anada, S. Hashimoto, *Adv. Synth. Catal.* **2005**, *347*, 1483–1487.

[4] R. P. Reddy, G. H. Lee, H. M. L. Davies, *Org. Lett.* **2006**, *8*, 3437–3440.

[5] K. M. Chepiga, C. Qin, J. S. Alford, S. Chennamadhavuni, T. M. Gregg, J. P. Olson, H. M. L. Davies, *Tetrahedron* **2013**, *69*, 5765–5771.

[6] J. R. Denton, K. Cheng, H. M. L. Davies, *Chem. Commun.* **2008**, 1238–1240.

[7] J. R. Denton, D. Sukumaran, H. M. L. Davies, *Org. Lett.* **2007**, *9*, 2625–2628.

[8] J. R. Denton, H. M. L. Davies, *Org. Lett.* **2009**, *11*, 787–790.

[9] C. Qin, V. Boyarskikh, J. H. Hansen, K. I. Hardcastle, D. G. Musaev, H. M. L. Davies, *J. Am. Chem. Soc.* **2011**, *133*, 19198–19204.

[10] J. M. Fraile, J. I. García, A. Gissibl, J. A. Mayoral, E. Pires, O. Reiser, M. Roldán, I. Villalba, *Chem. Eur. J.* **2007**, *13*, 8830–8839.

[11] D. T. Boruta, O. Dmitrenko, G. P. A. Yap, J. M. Fox, *Chem. Sci.* **2012**, *3*, 1589–1593.

[12] V. N. G. Lindsay, A. B. Charette, *ACS Catal.* **2012**, *2*, 1221–1225.

[13] a) P. Müller, A. Ghanem, *Org. Lett.* **2004**, *6*, 4347–4350; b) A. Ghanem, M. G. Gardiner, R. M. Williamson, P. Müller, *Chem. Eur. J.* **2010**, *16*, 3291–3295.

[14] A. Ghanem, H. Y. Aboul-Enein, P. Müller, *Chirality* **2005**, *17*, 44–50.

[15] F. G. Adly, J. Maddalena, A. Ghanem, *Chirality* **2014**, *26*, 764–774.

[16] J. T. Mattiza, J. G. G. Fohrer, H. Duddeck, M. G. Gardiner, A. Ghanem, *Org. Biomol. Chem.* **2011**, *9*, 6542–6550.

[17] T. P. Yoon, E. N. Jacobsen, *Science* **2003**, *299*, 1691–1693.

[18] A. DeAngelis, O. Dmitrenko, G. P. A. Yap, J. M. Fox, *J. Am. Chem. Soc.* **2009**, *131*, 7230–7231.

[19] a) R. Filler, Y. Kobayashi, *Biomedical Aspects of Fluorine Chemistry*, Elsevier Biomedical, Amsterdam, **1982**; b) J. T. Welch, S. Eswarakrishnan, *Fluorine in Bioorganic Chemistry*, Wiley, New York, **1990**; c) T. Hiyama, *Organofluorine Compounds, Chemistry and Applications*, Springer, New York, **2000**; d) D. O'Hagan, D. B. Harper, *J. Fluorine Chem.* **1999**, *100*, 127–133.

[20] a) R. D. Chambers, *Fluorine in Organic Chemistry*, Blackwell, Boca Raton, **2004**; b) M. Shimizu, T. Hiyama, *Angew. Chem. Int. Ed.* **2005**, *44*, 214–231; *Angew. Chem.* **2005**, *117*, 218–234.

[21] B. K. Park, N. R. Kitteringham, P. M. O'Niel, *Annu. Rev. Pharmacol. Toxicol.* **2001**, *41*, 443–470.

[22] B. E. Smart, *J. Fluorine Chem.* **2001**, *109*, 3–11.

[23] A. DeAngelis, D. T. Boruta, J.-B. Lubin, J. N. Plampin, G. P. A. Yap, J. M. Fox, *Chem. Commun.* **2010**, *46*, 4541–4543.

[24] V. N. G. Lindsay, W. Lin, A. B. Charette, *J. Am. Chem. Soc.* **2009**, *131*, 16383–16385.

[25] H. Tsutsui, T. Abe, S. Nakamura, M. Anada, S. Hashimoto, *Chem. Pharm. Bull.* **2005**, *53*, 1366–1368.

[26] S. Kitagaki, M. Anada, O. Kataoka, K. Matsuno, C. Umeda, N. Watanabe, S. Hashimoto, *J. Am. Chem. Soc.* **1999**, *121*, 1417–1418.

[27] a) T. M. McPhillips, S. E. McPhillips, H.-J. Chiu, A. E. Cohen, A. M. Deacon, P. J. Ellis, E. Garman, A. Gonzalez, N. K. Sauter, R. P. Phizackerley, S. M. Soltis, P. Kuhn, *J. Synchrotron Radiat.* **2002**, *9*, 401–406; b) W. Kabsch, *J. Appl. Crystallogr.* **1993**, *26*, 795–800.

[28] G. M. Sheldrick, *SHELX-97*, *Programs for Crystal Structure Analysis*, Universität Göttingen, Germany, **1998**.

[29] L. J. Barbour, *J. Supramol. Chem.* **2001**, *1*, 189–191.

[30] A. Spek, *J. Appl. Crystallogr.* **2003**, *36*, 7–13.

[31] a) H. Tomioka, H. Miyagawa, *J. Chem. Soc. Chem. Commun.* **1988**, 1183–1184; b) H. M. L. Davies, G. H. Lee, *Org. Lett.* **2004**, *6*, 2117–2120.

[32] H. M. L. Davies, S. A. Panaro, *Tetrahedron Lett.* **1999**, *40*, 5287–5290.

[33] H. M. L. Davies, P. R. Bruzinski, D. H. Lake, N. Kong, M. J. Fall, *J. Am. Chem. Soc.* **1996**, *118*, 6897–6907.

[34] D. T. Nowlan, T. M. Gregg, H. M. L. Davies, D. A. Singleton, *J. Am. Chem. Soc.* **2003**, *125*, 15902–15911.

Received: November 30, 2015
Published online on February 2, 2016